

UC Santa Cruz

UC Santa Cruz Electronic Theses and Dissertations

Title

Lichen as a Bioindicator of Atmospheric Mercury Deposition and Emissions: A Study of the Sulphur Bank Mercury Mine and New Almadén Mercury District

Permalink

<https://escholarship.org/uc/item/41814090>

Author

Rothman, Michelle Rose

Publication Date

2024

Peer reviewed|Thesis/dissertation

UNIVERSITY OF CALIFORNIA
SANTA CRUZ

**Lichen as a Bioindicator of Atmospheric Mercury Deposition and
Emissions: A Study of the Sulphur Bank Mercury Mine and New
Almadén Mercury District**

A thesis submitted in partial satisfaction
of the requirements for the degree of

MASTER OF SCIENCE

in

EARTH SCIENCES

by

Michelle Rothman

June 2024

The Thesis of Michelle Rothman
is approved:

Associate Researcher Peter Weiss-Penzias

Professor Carl Lamborg

Professor Adina Paytan

Peter Biehl
Vice Provost and Dean of Graduate Studies

Table of Contents

1. Introduction
 - 1.1 Mercury
 - 1.2 New Almadén Quicksilver Mining District
 - 1.3 Sulphur Bank Mercury Mine
 - 1.4 The Release of Mercury into the Environment through Mine Waste
 - 1.5 Lichen as a Bioindicator
 - 1.6 Using Lichen Transplants as Active Bioindicators of Atmospheric Mercury
 - 1.7 Objectives and Goals
2. Methods
 - 2.1 Study Areas
 - 2.1.1 Transplantation Experiment at New Almadén Mining District
 - 2.1.2 Mercury Passive Air Samplers
 - 2.1.3 Sulphur Bank Mercury Mine
 - 2.2 Total Mercury Analysis
 - 2.3 Data Analysis
 - 2.4 Geo Statistical Analysis
3. Results
 - 3.1 Transplantation Experiment
 - 3.1.1 THg Accumulation

- 3.1.2 THg Release
 - 3.1.3 THg in Controls
 - 3.1.4 MerPAS Results
 - 3.2 Sulphur Bank Mercury Mine
 - 3.2.1 Total Mercury Concentrations in Lichens within SBMM and the Surrounding Areas
 - 3.2.2 Total Mercury Concentrations by Lichen Species
- 4. Discussion
 - 4.1 Lichen as a Bioindicator
 - 4.2 THg Accumulation and Release by Transplanted Lichens at NAMD
 - 4.2.1 Effect of Lichen Species on THg Accumulation
 - 4.2.2 Hg Emission Hotspots at NAMD
 - 4.2.3 THg Release
 - 4.3 Hg Pathways at SBMM
- 5. Conclusion
 - 5.1 Impact of Research
 - 5.2 Future Studies
- 6. Bibliography

List of Figures

1. Study Areas
2. Transplantation Shields
3. Shield Locations at New Almadén Mining District
4. Shield Locations in Comparison to a Heat Map of THg Concentrations
5. MerPAS Method
6. Clear Lake and the Herman Impoundment
7. Hg Uptake at Mine Hill
8. Hg Uptake at Almadén Reservoir
9. Hg Uptake at Hacienda/Deep Gulch
10. Rate of THg Uptake by Lichen Species
11. Kinetic THg Release at Lexington Reservoir
12. Kinetic THg Curves for Control Species at Mine Hill
13. Kinetic THg Curves for Control Species at Almadén Reservoir
14. Kinetic THg Curves for Control Species at Hacienda/Deep Gulch
15. Kinetic THg Curves for Control Species at Lexington Reservoir
16. Scatterplot of Daily Rates of THg Accumulation vs Hg Air Concentration
17. Maps of Daily Rates of THg Accumulation and Hg⁰ Air Concentration
18. Map of Sampling Locations at Clear Lake
19. Heat Map of THg Concentrations at SBMM
20. Bar Graph of Tailings/South Waste Rock Pile THg Concentrations by Species
21. Bar Graph of Satellite Waste Rock Pile THg Concentrations by Species

22. Bar Graph of North Waste Rock Pile THg Concentrations by Species

List of Tables

1. Summary of Linear Regression Statistics
2. Summary of MerPAS Results

Abstract

Lichen as a Bioindicator of Atmospheric Mercury Deposition and Emissions: A Study of the Sulphur Bank Mercury Mine and New Almadén Mercury District

Michelle Rothman

Mercury, a highly toxic heavy metal, remains of global concern due to its capacity to cause significant harm to human health and the environment. Mercury (Hg) can travel long distances within the atmosphere, bioaccumulate in living organisms, and act as a potent neurotoxin. Mercury contamination remains a prevalent issue due to historic mining practices, as it was once mined for various industrial applications and for its ability to form a gold amalgam. Large amounts of mine waste, also known as calcines, remain at historic mercury mines, representing significant sources of Hg emissions to the local environment through wet and dry atmospheric deposition. Even though the presence of mercury contamination at these abandoned mines has been documented, there is a notable gap in our understanding of how mercury emissions from mine waste can contaminate the environment through atmospheric transport. This study aims to investigate the spatial and temporal environmental impacts of Hg emissions and determine atmospheric pathways of contamination from mine waste at the New Almadén Mining District (NAMD) and the Sulphur Bank Mercury Mine (SBMM) in Northern California. However, traditional methods of monitoring atmospheric mercury present challenges due to the high cost of equipment and the temporal and spatial variability of air pollution. So, in this study, we employed lichen as a bioindicator of atmospheric mercury emissions due to its abundance in the study area, low cost, and past success in using lichen to record Hg. Measuring total mercury concentrations across various lichen species and locations at the NAMD and the SBMM allowed

us to identify Hg emission hotspots and provide valuable insights into the spatial and temporal distribution of Hg in a contaminated environment. The concentration of total mercury in lichen samples reached 45 ppm at the Sulphur Bank Mercury Mine, indicating significant levels of contamination in historic calcine processing areas.

Acknowledgments

Thank you, Santa Clara Valley Water District, for the funding and support

Thank you, Dr. Peter Weiss-Penzias, for your mentorship, patience, and sharing your knowledge

Thank you, Santa Clara County Parks District, for the sampling permits

Thank you, USGS Mercury Lab in Madison, WI, for equipment and sample analysis

Thank you, Charlie Alpers, for your guidance and assistance at the Sulphur Bank Mercury Mine

Thank you, Millhauser Lab and Lamborg Lab for allowing me to use your facilities and
equipment

Thank you, Nettie Calvin, for all of your help, patience, and mentorship

Thank you, undergraduate Elizabeth Pechullis, for your assistance in field sampling, sample
preparation, and GIS

Thank you, undergraduates Kit Vu, Matthew Geller, Molly Hoffman, and Vanessa Pham for all
of your help this past year

Lichen as a Bioindicator of Atmospheric Mercury Deposition and Emissions: A Study of the Sulphur Bank Mercury Mine and New Almadén Mercury District

Michelle Rothman

1. Introduction

1.1 Mercury

Mercury is a highly toxic contaminant of global concern due to its ability to bioaccumulate in the food chain and linger in the environment, posing risks to ecosystems and human health. Mercury is a naturally occurring element within Earth's biogeochemical system and can be released into the atmosphere through natural and anthropogenic sources¹. Volcanic activity, forest fires, rock weathering, and soil emissions are all natural sources of mercury emissions^{2,3}. Anthropogenic sources of mercury include coal-fired power plants, fossil fuel combustion, non-ferrous metal production, waste incineration, abandoned mercury mines, and artisanal gold mining^{4,5}. Over centuries of anthropogenic activity, mercury has been introduced into the atmosphere, leading to both wet and dry Hg deposition into aquatic ecosystems⁶.

Mercury exists in many forms and oxidation states, primarily as elemental mercury (Hg^0), divalent inorganic mercury (Hg^{2+}), and organic mercury compounds (MeHg)^{2,3}. Gaseous elemental mercury (Hg^0), the most abundant form of mercury in the atmosphere, is considered a global-scale pollutant due to its long residence time

and ability to be transported over long distances^{1,4,7}. Elemental mercury (Hg^0) can be oxidized to form the highly reactive divalent mercury (Hg^{2+})⁴. In aquatic environments, inorganic mercury (Hg^{2+}) can be methylated by sulfate- and iron-reducing bacteria, producing methylmercury (MeHg)^{8,9}. Methylmercury (MeHg) is a highly toxic form of mercury that is of concern due to its ability to pass through the blood-brain and placental barriers and bioaccumulate in food chains, resulting in elevated concentrations found in top predators within aquatic ecosystems^{3,8,9}. Long-term and low-dose exposure to methylmercury can result in severe damage to the central nervous system, as well as the kidney, liver, cardiovascular, and immune systems⁹. In 2013, the Minamata Convention was agreed upon by over 140 countries to address the consequences of mercury exposure to human health and the environment by reducing global Hg emissions^{9,10}.

In the San Francisco Bay Area, mercury contamination remains a prevalent issue due to historic mining practices. Mercury was used in small and large-scale gold mining to separate and purify gold from ore due to its ability to form an amalgam^{2,11}. The mercury used in the gold recovery process was primarily obtained from mines in the California coast range on the west side of the Central Valley^{2,12}. Mercury is recovered from the chief mineral ore Cinnabar (HgS) in the process known as calcination. The calcination process involved heating the cinnabar ore in a retort or rotary furnace, and then extracting and condensing elemental mercury vapor. Mercury calcination is considered an inefficient process, and poor-quality unroasted ore and roasted ore residues were dumped in the surrounding environment¹³. These mercury-

enriched ore deposits, also known as calcines, present a significant source of mercury emissions to the local environment and atmosphere. Calcines can also release Hg into nearby aquatic ecosystems through erosion and leaching¹⁴. The mercury species in these deposits include metacinnabar, elemental mercury, mercury sulfates, and mercury chlorides^{15,16}. Significant amounts of calcines remain at Hg mining sites after the California gold rush, contaminating aquatic ecosystems and leading to atmospheric mercury emissions^{2,16}.

1.2 New Almadén Quicksilver Mining District

In 2000, the United States Geological Society reported that about 550 abandoned and inactive mercury mines in California continued to cause significant environmental harm². The New Almadén Quicksilver Mining District (NAQ) in Santa Clara County, California, stands out as having been North America's largest and most productive mine. Mercury production on a commercial scale began at the New Almadén Mine in 1846 until its closure in the mid-1970s¹⁷. Once the largest mercury producer in the United States, the New Almadén mine produced 38,000 metric tons of mercury, or 5 percent of the world's total mercury, through 1977^{17,18}. In 1975, the mine closed and was sold to the Santa Clara County Parks and Recreation Department for recreational use, now known as Almadén Quicksilver County Park¹⁹. The park has undergone remediation at five former mercury processing areas from 1998-2000, and the implementation of the Hacienda and Deep Gulch Calcines Remediation Project began in October 2022²⁰. New Almadén Mining District is

located in the watershed of the Guadalupe River, which drains into South San Francisco Bay through the Alviso Slough. Even with current remediation efforts, calcine deposits continue to pollute the surrounding environment and the San Francisco Bay through the transport of mercury-enriched sediment and leaching of mine waste into waterways^{2,21}.

Atmospheric monitoring of Hg around mining areas is crucial to understanding the complex dynamics of Hg transport and its potential impacts on the environment. Numerous studies have been performed to measure mercury emissions from highly productive mining areas, including the Almadén mines in Spain and the Idrija mines in Slovenia^{13,22,23}. These studies found that the local environment surrounding former mercury mines demonstrated high levels of mercury contamination. In a study conducted by Jiménez-Moreno et al, they found that the Hg isotope composition in lichens surrounding mines at the Almadén mining district revealed that both the atmosphere and rivers are significantly impacted by Hg released from the mines²³. Considering how productive the New Almadén Mining District once was, there is a surprising absence of studies actively monitoring atmospheric mercury emissions around the mine. The lack of prior air monitoring studies at this location represents a gap in our understanding of the extent of mercury contamination.

1.3 Sulphur Bank Mercury Mine

Similar challenges of mercury contamination stemming from mine waste persist at the Sulphur Bank Mercury Mine, once one of the largest producers of mercury in California. The Sulphur Bank Mercury Mine is a 160-acre abandoned open-pit mercury mine situated on the south shore of the Oaks Arm of Clear Lake in Lake County, California²⁴. The Sulphur Bank Mercury Mine experienced intermittent mining operations for sulfur and mercury from 1865 to 1957²⁵. During this period, mining operations removed between 4400 and 7000 metric tons of Hg recovered from 2.5 million cubic yards of mine waste^{24,25}. On-site, a 23-acre flooded open-pit mine exists, referred to as the Herman Impoundment²⁴. The Herman Impoundment is inundated with mine waste, polluted water, and geothermal groundwater naturally containing mercury and arsenic²⁴. Mining activities at the Herman Impoundment have led to the dispersal of calcines across the region, eventually ending up in Clear Lake²⁴. The disposal of mine waste has led to the contamination of soils, surface water, and groundwater in the area, releasing hazardous contaminants such as mercury, arsenic, and antimony, thereby posing risks to human health²⁴. Mercury contamination threatens the Elem Indian Colony, located adjacent to the Herman Impoundment, who rely on Clear Lake's food and water resources. Stormwater and groundwater movement of mercury from mine waste have resulted in mercury-enriched sediment at the bottom of the lake, which has accumulated in fish over time²⁴. In 1987, the California Office of Environmental Health and Hazard Assessment (OEHHA) issued a fish consumption advisory due to elevated mercury

concentrations in fish²⁴. In 1990, the Sulphur Bank Mercury Mine became an Environmental Protection Agency (EPA) superfund site and has undergone various cleanup efforts to minimize the site's impact on human health and the environment²⁴. The EPA is currently working with the Elem Indian Colony, the greater Clear Lake community, the United States Geological Survey (USGS), and the Tribal nations to distinguish natural sources of mercury from mine waste mercury, reduce mercury entering Clear Lake, remove and cover contaminated residential soils, and clean up the waste piles in a finalized plan²⁴. Clear Lake is currently used for recreational activities including fishing and swimming, as the mercury levels in the lake water comply with government standards²⁴.

1.4. The Release of Mercury into the Environment through Mine Waste

Calcines can release mercury into the environment through mercury vapor emitted into the atmosphere, mercury-contaminated soils, and mine drainage. The dumping of calcines can contaminate soil, resulting in atmospheric emissions of elemental mercury through volatilization and wind entrainment of Hg bound to dust particles^{14,26}. Total mercury concentration in soil, soil temperature, light energy, rainfall, and vegetation can influence the amount of Hg emitted from soil²⁷. Mercury emitted from calcines and contaminated soils to the atmosphere can be re-deposited to terrestrial and aquatic environments through wet and dry deposition¹⁶. Additionally, mercury-contaminated soils at mine sites are a source of ionic and elemental mercury that can be transported and subsequently converted to methylmercury in downstream

aquatic environments through surface runoff¹⁶. Mercury can be mobilized into aquatic environments when contaminated soil becomes saturated by rainfall and then eroded by overland flow into tributaries¹⁴. Another source of mercury and methylmercury can be mine drainage, created when rainwater or groundwater mixes with waste extracted primarily through underground mining methods¹⁶. Acidic mine drainage can provide a favorable environment for mercury methylation by sulfate-reducing bacteria due to the high concentration of sulfate added as sulfuric acid in the process¹⁶. The formation of sulfuric acid results from the chemical reaction of surface water and shallow subsurface water with rocks that contain sulfur-bearing minerals²⁸. The release of mercury from calcines and contaminated soils, along with the formation of mine drainage, demonstrates the need for more research at these abandoned mine sites to mitigate the risks to human health and the environment. When observing mercury-contaminated sites, mercury fluxes to water are often prioritized due to the direct correlation with methylation and bioaccumulation in downstream aquatic ecosystems¹⁴. However, understanding the complex dynamics of atmospheric Hg emissions around mining areas is imperative for assessing their impact on environmental and human health. The emissions of elemental Hg through volatilization around mining areas can contribute to the global atmospheric pool due to the long atmospheric lifetime of Hg¹⁴. Hg emissions originating from mining areas can eventually be re-deposited, methylated, and accumulated in aquatic and terrestrial organisms¹⁴. Additionally, observations have shown that the release of mercury from contaminated sites has increased mercury concentrations in the local ambient air,

posing a risk to human health when inhaled¹⁴. Atmospheric Hg monitoring is needed to accurately determine the transport and fate of airborne Hg emissions around mining areas. With more data, the full scope of exposure risks facing nearby communities and ecosystems can be assessed. However, traditional air sampling methods present difficulties due to the high cost of equipment, the risk of theft or vandalism, and the temporal and spatial variability of air pollution which may require multiple monitoring sites.

1.5 Lichen as a Bioindicator

Lichens are a symbiosis composed of a fungus (mycobionts) and green algae or cyanobacteria (photobionts). The fungi provides the algae with protective sheltering structures, while the algae supplies photosynthetically fixed carbon as an energy source²⁹. Lichens are ubiquitous, as they are perennial organisms and can grow nearly in all habitats. Lichens primarily receive nutrients from the atmosphere as they lack a vascular and root system³⁰. Unlike vascular plants, lichens do not possess a waxy cuticle, nor structures specialized for the transport of minerals, water, and food. The lack of protective cuticles and specialized structures allows lichens to accumulate atmospheric nutrients and metals that are required from metabolism across the thallus surface. The process also results in the uptake of heavy metals in proportion to their environmental concentrations³¹. It has been observed that lichens accumulate pollutants through extracellular cation exchange in the cell wall and on the plasma membrane surface³². Lichens can also accumulate insoluble particulate

matter in the thallus in proportion to the environmental availability of particles and duration of exposure^{32,33}. These unique properties of lichens allow them to be one of the best and most reliable options to serve as bioindicators of air pollution.

The use of lichens as bioindicators to measure inorganic and organic air pollutants has been well documented.^{30,31,34} One way that lichens act as bioindicators is through their susceptibility to pollution, where the absence of sensitive species, decreased diversity, and observable morphological, anatomical, and physiological alterations are taken as evidence of the presence of significant amounts of pollution³⁵. Lichens have been recognized as an indicator of air quality since 1866 by the Finnish lichenologist W. Nylander, who observed that lichens showed incomplete development near urban areas in Paris³⁶. In recent decades, lichens have been one of the most used bioindicators to measure air pollution, particularly heavy metals such as mercury³⁷. Studies carried out by Jiménez et al (2016) and Berdonces et al. (2017) used lichen as a bioindicator to measure mercury concentrations at the Almadén mercury mining district in Spain. Both of these studies used lichen to identify “hot spots”, and the fate of mercury contamination using Hg isotope signatures in lichens in the Jiménez et al (2016) experiment and comparing mercury concentrations in air with respect to mercury concentrations in lichen in the Berdonces et al. (2017) study^{22,23}. Past research has demonstrated that different lichen species in the same location can contain various concentrations of metals, attributed to differences in morphological and structural features³¹. A study conducted by Garty (2001) revealed that the extent of surface area in lichen species can impact the distribution of heavy

metals³¹. For example, foliose lichens are characterized by an equal-sized surface as they have a leaf-like thallus and flattened lobes, and can therefore promote a uniform accumulation of heavy metals^{31,38}. There have also been reports of significantly higher heavy metal concentrations in the inner, older areas of the thalli than in the peripheral areas of foliose native lichens at contaminated sites, suggesting that the age of the thallus may influence the accumulation of heavy metals^{37,39}.

Lichens can provide significant benefits over other methods of air sampling. Lichens can serve as an inexpensive air sampling method as they are abundant over a wide geographical range and relatively easy to collect⁴⁰. Lichens can be available for monitoring throughout the year and are tolerant to extreme environmental conditions³¹. In addition, lichens can allow assessment of long-term air pollution accumulation as many species can accumulate high levels of pollutants in their thalli without exhibiting damage⁴⁰. Lichens can be particularly useful in monitoring the air quality of remote areas with limited road access and electricity. In this study, we used epiphytic fruticose lichens as a bioindicator to measure atmospheric mercury emissions due to their abundance in the study area, low cost, and past success in the field. However, interpreting Hg concentrations in lichen can present difficulties due to the influence of climatic and environmental conditions, impacting metabolic growth rate and the deposition and bioavailability of Hg³⁷.

1.6 Using Lichen Transplants as Active Bioindicators of Atmospheric Mercury

Lichen transplants can serve as a creative technique for the biomonitoring of airborne pollutants, particularly heavy metals such as mercury. The methodology for lichen transplantation experiments involves transferring lichens from an uncontaminated site to a contaminated area, followed by measurements of pollutant uptake through subsampling of the transplanted lichens at different intervals.

Additionally, reverse lichen transplantation studies have been conducted, where lichens from a contaminated site are transplanted to an uncontaminated location, allowing for the measurement of pollutant release over time⁴¹. In recent years, lichen transplant studies have become increasingly popular as lichens are relatively inexpensive and easy to transport, the monitoring sites can be chosen, and the initial elemental concentration and exposure time are known beforehand⁴².

Extensive research has been conducted to explore the uptake of airborne pollutants in lichen transplant experiments. In a study performed by Lopez-Berdonces et al (2017), multiple lichen species were transplanted from an uncontaminated site to the Almadén mercury mining district (AMMD) in South Central Spain, once one of the world's most productive mercury mines²². The authors sampled the transplanted lichens at various intervals: 10, 45, and 92 days²². The authors found differences in the uptake rate based on the lichen species sampled and measured high mercury uptake rates in the lichens closer to known sources of mercury emissions²². It was also noted that the mercury concentrations in lichens reach an equilibrium with mercury in air, based on their additional mercury gas samples collected using a

LUMEX RA-915p²². The accumulation of mercury was represented in a first-order kinetic model, utilizing the ratio of measured mercury concentrations at each time point to the initial mercury concentrations in transplanted lichen²². Furthermore, a lichen transplant study by Loppi et al (1998) measured the accumulation of trace metals (Cd, Cr, Cu, Pb, and Zn) in the lichen species *Evernia prunastri*. The authors transplanted the epiphytic (tree-growing) lichen species from an unpolluted area to the urban environment of Teramo in Central Italy, subsampling and analyzing the lichen every two months over a year-long period³². It was found that concentrations of trace metals were statistically higher in transplanted lichens than in control samples after only two months, ultimately revealing that the elements in question polluted the transplanted lichens³².

While the monitoring of pollutant uptake has been studied in lichen transplant experiments, there has been comparatively less focus on documenting the release of airborne pollutants in lichen. However, one study conducted by Vannini et al (2021) investigated both the accumulation and release of the ionic form of mercury in lichens, using the lichen species *Evernia prunastri*⁴¹. The authors collected native lichen from a remote area in Tuscany of central Italy, incubated the lichens with solutions containing Hg²⁺ at different concentrations, and then transplanted them to another location free of local mercury contamination. The authors found that the transplanted lichens accumulated mercury proportionally to the incubation concentrations and then released mercury over time, eventually decreasing to stable concentrations after 6-24 months⁴¹. The results of that study provided valuable

insights into the dynamics of the uptake and release of mercury over time, demonstrating how lichens can exhibit different concentrations of mercury depending on temporal and spatial changes.

These studies demonstrate how lichen transplantation experiments can offer advantages in determining the transport and emissions of atmospheric mercury in contaminated areas. Measuring mercury uptake in transplanted lichens can provide accurate spatial and temporal patterns of Hg contamination around emission sources²³. Reverse transplant experiments can provide insight into the amount of mercury released over time once accumulated in lichens, reflecting the decreasing environmental availability of Hg in the surrounding environment²³.

1.7 Objectives and Goals

The main objectives of this study are to investigate the spatial and temporal environmental impacts of Hg emissions and determine atmospheric pathways of contamination from mine waste at the New Almadén Mining District and the Sulphur Bank Mercury Mine in California. At NAMD, we aimed to identify and measure Hg emission sources and deposition by utilizing lichen as a bioindicator for atmospheric mercury in a transplantation study. Conducting a lichen transplantation experiment at the NAMD allowed us to quantify the Hg uptake and release rate over time in transplanted lichens. We also determined how site location and the lichen species used impact Hg accumulation and release.

At the EPA Superfund Sulphur Bank Mercury Mine (SBMM), our goal was to gain a better understanding of the transport of atmospheric Hg in a contaminated environment. We accomplished this goal by identifying elevated gaseous mercury emissions and deposition using native epiphytic lichens. We collected lichens from various locations where calcines were present, including background lichens free from mercury contamination to represent a control.

2. Methods

2.1 Study Areas

2.1.1 Transplantation Experiment at New Almadén Mining District

A lichen transplantation experiment was conducted to investigate the accumulation and release of mercury over time using selected lichen species at various sites in the New Almadén Mining District (NAMD). Former Masters students, Bella Zheng and Brittany Straw, conducted multiple experiments using native lichens to identify hotspots of mercury contamination at NAMD. Their findings helped us determine where to transplant the lichen, as we aimed to position them in areas exhibiting elevated mercury concentrations. We collected three lichen species, *Evernia prunastri*, *Ramalina leptocarpha*, and *Usnea* sp., from the background area at Lexington Reservoir. *Ramalina leptocarpha* was the most abundant species collected at Lexington Reservoir, allowing it to be transplanted to every site. The Lexington Reservoir is an artificial lake on the Los Gatos Creek near

Los Gatos, California and is determined to be free from local Hg contamination⁴³. Lichens were collected from mainly Oak tree branches with heavy lichen growth at the Lexington Reservoir, with species identified using a field guide. The collected lichens were then rinsed using spring water, separated by species, pat-dried with KayDries, and placed into acid-cleaned nylon mesh bags. We chose to use spring water instead of deionized water to rinse the lichens, as deionized water could leach nutrients out from the lichen and potentially damage our samples. The lichens were spread out in the mesh bags to promote airflow. The lichen bags were then hung in rain shields from tree branches at 8 different sites in the New Almadén Mining District demonstrated in Figure 1, including three sites at Mine Hill near Englishtown, two sites near Almadén Reservoir, two sites in the Hacienda Furnace Yard, and one site in the Deep Gulch area (Figure 3). At each site, four lichen bags were hung below a shield to protect the samples from rain. Transplantation shields 1-5 consisted of three bags of each lichen species from Lexington to measure mercury uptake and one control bag. Transplantation shields 7-9 located in the Hacienda/Deep Gulch area consisted of three bags of only *Ramalina leptocarpha*, in addition to one control bag. The control bags consisted of native lichens gathered from each respective shield location. The control bags helped us assess if there were any changes in the health of the lichens resulting from transplantation, as well as any changes in the uptake or release of mercury. The bags were hung from oak trees approximately 1.5 m off the ground, hidden in dense foliage and invisible from trails nearby to prevent vandalism.

In addition to measuring mercury uptake, we also conducted a reverse transplantation experiment to quantify the release of mercury in lichens. Lichens were collected from various locations in Mine Hill, the Hacienda Furnace yard, and the Deep Gulch area. The lichens were then transplanted to the Lexington reservoir, our background site. The same sampling and transplantation protocols were used in the reverse transplantation experiment. However, only two shields were placed at the same site near the Lexington Reservoir, as demonstrated in Figure 2. Each shield contained three transplanted lichen bags and one control bag, with the control consisting of lichen collected at Lexington reservoir.

After the shields were deployed, subsamples of each species in each bag were collected to represent the initial time point. Approximately every 30 days, we returned to subsample the bags for 6-7 months. About 2-5 grams of lichen was collected from each bag, ensuring that there was a sufficient supply of lichen to sustain the experiment for an extended period.

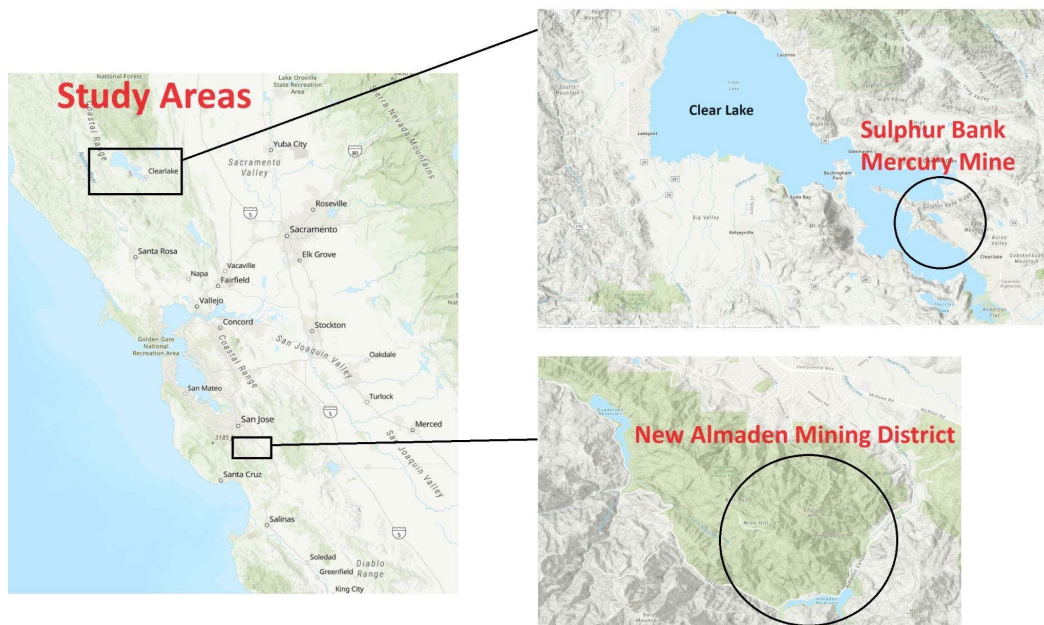


Figure 1: Map showing the location of the two study areas, the New Almadén Mining District (NAMD) and the Sulphur Bank Mercury Mine (SBMM).



Figure 2: An example of the equipment used for transplantation experiments, depicted at NAMD. This photo and approach were developed by Straw (2023)⁴⁴. Each site contained a shield with 4 mesh bags of lichen suspended from it.

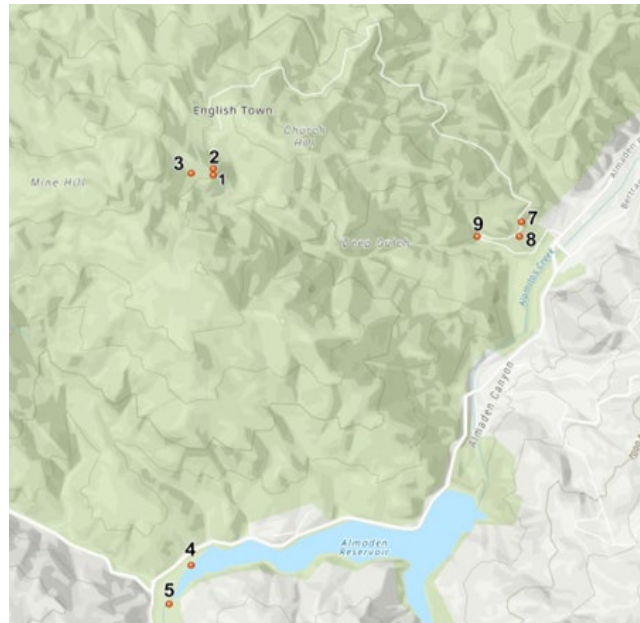


Figure 3: A map indicates each transplanted site's location in the New Almadén Mining District. These shields were transplanted from the Lexington Reservoir. Shields 1-3 are located in Mine Hill, 4-5 are near Almadén Reservoir, 7 in the Deep Gulch area, and 8-9 are in the Hacienda Furnace Yard.



Figure 4: A map indicates each transplanted site's location compared to a heat map, obtained from Brittany Straw's master's thesis⁴⁵. This map was made with ArcGIS's Empirical Bayesian Kriging analysis tool, using THg concentrations from 238 lichen samples. The heatmap shows low average THg levels in blue and high average THg levels in red. Shields 1-3, 4-5, and 7-9 were transplanted from the Lexington Reservoir to the New Almadén Mining District (NAMD). Shields 6 and 10 were transplanted from NAMD to the Lexington Reservoir.

2.1.2 Mercury Passive Air Samplers

Two Mercury Passive Air Samplers (MerPAS) from the Tekran Corporation were installed alongside each lichen transplantation shield at NAMD. Supplementing our lichen measurements with the MerPAS allowed us to investigate the potential correlation between the air concentration of elemental mercury and the THg concentrations and uptake rate of Hg in the lichens. MerPAS are a power-free passive air sampling method that uses an activated carbon sorbent to sample Hg in ambient air⁴⁵. Briefly, gaseous elemental Hg enters the sampler and diffuses at a known rate into a chamber where it is trapped on a sulfur-impregnated carbon sorbent⁴⁶. The carbon sorbent is contained in a stainless-steel mesh cylinder that is inserted into a porous polyethylene diffusive barrier, controlling the rate of diffusion from the air to the sorbent⁴⁶. This diffusive barrier is then inserted into a protective plastic jar that eliminates the impacts of wind and solar radiation and can be used as a container for transport⁴⁵. The MerPAS were deployed in duplicates at each lichen transplant location to assess variance and ensure analytical replication. The MerPAS were installed on trees near the transplantation shields, approximately 1.5 m off the ground. Each MerPAS was left in the field and sampled ambient air for 60 days. After 60 days, the MerPAS were uninstalled and mailed to the USGS in Madison, WI for further analysis. The carbon sorbent was then analyzed in a Direct Mercury Analyzer following US EPA method 7473, where total Hg was determined. Gaseous Hg

concentrations in the atmosphere, C (ng/m^3), are calculated from the following equation:

$$C = \frac{m}{(SR * t)} \quad (1)$$

where m is the mass of sorbed Hg (ng), SR is the sampling rate of the PAS ($\text{m}^3 \text{ day}^{-1}$) and t is the deployment time of the sampler (days). We used a sampling rate of $0.111 \text{ m}^3 \text{ day}^{-1}$ as recommended by the Tekran Corporation^{46,47}



Figure 5: An example of the installation of the MerPAS, depicted at NAMD. This photo and approach were developed by Straw (2023)⁴⁴. Alongside every shield, 2 air collectors were installed approximately 1.5 m off the ground and left in the field for about 60 days.

2.1.3 Sulphur Bank Mercury Mine (SBMM)

We used native epiphytic lichen to identify hotspots of gaseous mercury emissions and deposition originating from mine waste at the Sulphur Bank Mercury Mine (SBMM). In March of 2022, preliminary lichen sampling at the SBMM revealed extremely high total Hg concentrations of up to 23 ppm, and lower, but still elevated total Hg concentrations of 1 ppm at the shore of Clear Lake. In May of 2023, we returned to the SBMM to collect lichen samples from various locations around Herman Impoundment where waste rock is present and in areas with known contamination. Lichens were collected from the North Waste Pile, South Waste Pile, West Waste Pile, West Ore Pile, a tailings pile where calcines used to be processed in a furnace plant, and from the west shoreline of the Herman Impoundment where hydrothermal vents are present. We collected multiple lichen species, including *Evernia prunastri*, *Ramalina leptocarpha*, *Usnea sp.*, *Ramalina farinacea*, and *Ramalina menziesii*, all visually identified with the assistance of a comprehensive field guide. The selection of lichen species for this study was based on their abundance in the area as well as ease of visual identification. Various lichen species were collected to investigate potential variations in sensitivity to total mercury (THg) based on species and morphological traits.

Additional lichen samples were collected in background locations to represent controls. Ukiah, Nice, Cole Creek, Middle Creek, and Kelsey Creek are the areas we used as control sites. These locations are all in Northern California, with some close

by to Clearlake. Sampling these areas helped us determine the extent of mercury contamination originating from the SBMM at Clear Lake.



Figure 6: Figure 6A shows a photograph of Clear Lake in the distance captured in May of 2023. Figure 6B shows a photograph of the Herman Impoundment at Clear Lake, captured in May of 2023. Mining scars are visible along the shore of the Herman Impoundment.

2.2 Sampling Procedure

The coordinates of each sampling location were recorded using GPS and Google Maps. Samples were collected using trace-metal clean sampling techniques EPA Method 1669, clean hands-dirty hands, cleaning of tools with methanol between samples, and sample storage in two polyethylene storage bags⁴². Once the subsamples were placed into Ziploc bags, they were kept at ambient temperature when

transported back to the laboratory. At the laboratory, the samples were promptly stored in a freezer awaiting analysis.

2.3 Sample Preparation

After being removed from the freezer, lichen samples were inspected, identified, and separated by species. The approximate species composition of each sample was recorded. All foreign materials, such as tree bark, leaves, insects, and other plants, were removed from the lichen samples. Samples separated by species were then homogenized with liquid nitrogen to flash freeze the lichen and crushed using an acid-washed mortar and pestle. Samples were stored in a 50 mL polypropylene tube and then freeze-dried in a lyophilizer for 24 hours. Until analysis, the samples were placed back in the freezer at 4 °C.

2.4 Total Mercury Analysis

Total mercury concentrations (THg) were measured using direct mercury analyzer atomic absorption spectroscopy (DMA-80) (Milestone Corp.) following EPA method 7473⁴⁸. Approximately 0.01-0.05 grams of the dried lichen samples were scooped onto quartz and nickel sample boats and placed into the DMA-80. Lichen samples were analyzed in duplicates and were calibrated with liquid NIST Hg standards and Certified Reference Materials (CRM). Dogfish liver (DOLT-3) and peach leaves (SRM peach) were used for QA/QC. The mean recovery of THg in DOLT-3 was $102 \pm 2.9\%$ (N = 24) and $92 \pm 39\%$ (N = 18) for SRM peach leaves.

Certified Reference Materials (CRM) were used to assess the accuracy of the DMA between consecutive runs of <10 samples. Once the lichen samples were placed into the DMA-80, the samples were thermally decomposed in an oxygen-rich furnace and all mercury species in the samples were reduced to elemental Hg⁴⁹. The released elemental Hg is trapped through gold amalgamation. The system is purged and the amalgamator is subsequently heated, releasing all mercury vapor⁴⁹. The mercury vapor is then analyzed using a fixed wavelength atomic absorption spectrophotometer⁴⁹.

2.5 Data Analysis

All statistical tests were performed using R (4.3.2)⁵⁰. To determine the rates of mercury accumulation and release in transplanted lichens at NAMD, we first averaged the duplicate concentrations measured by the DMA-80. The averaged total mercury concentrations were then fitted into a first-order kinetic model, a method used by Lopez-Berdonces et al (2017) to measure mercury accumulation in lichen over a long exposure time²². The rate constant of mercury accumulation and release in the lichen can be described in the ratio as follows:

$$\text{Rate Constant} = \frac{q_L}{q_L^0} \quad (2)$$

where q_L is the lichen mercury concentration at a specific time and q_L^0 is the initial mercury concentration measured at the start of the transplantation experiment. The q_L^0 value was obtained by averaging several initial mercury concentrations from the same lichen species at different shield locations. We chose to average the initial

mercury concentrations from different shield locations to reduce variability and normalize the data. Linear regression tests were performed to determine if the lichen's exposure duration significantly influences the ratio between the lichen mercury concentrations at each time (q_L) and its initial mercury concentration (q^0_L). Linear regression analyses were conducted individually for each bag within transplantation shields 1-6 and 10, as they contained different species. Due to shields 7-9 comprising the same species in the mercury uptake bags, only one linear regression was performed for each shield. An ANOVA test was performed to determine if the rate of mercury accumulation differed significantly between each lichen species. Furthermore, a Pearson's linear correlation test was conducted to assess the correlation between the concentration of Hg^0 in the MerPAS and the slopes of daily kinetic THg accumulation in *Ramalina* lichen across transplants 1-5, 7-9, as well as the control lichen from shield 6.

Duplicates of total mercury concentrations were also averaged for the lichen samples at the SBMM. Nonparametric tests were performed due to the non-normality of the data. A Kruskal-Wallis test was conducted to determine if THg concentrations differed significantly between the lichen species sampled at SBMM.

2.6 Geostatistical Analysis

The ArcGIS Pro Geostatistical Analyst Interpolation tool, Empirical Bayesian Kriging (EBK), was used to create a map demonstrating the spatial distribution pattern of THg at the SBMM. Empirical Bayesian kriging is an interpolation

technique, meaning it is used to estimate unknown values that fall within the range of known data points. It makes these predictions more accurate by considering potential errors in the data patterns through multiple simulations⁵¹. Unlike other kriging methods requiring one to adjust parameters manually, EBK automatically calculates these parameters through subsetting and simulations⁵¹. This automatic process helps ensure the results are more reliable and less subjective.

The data underwent log empirical transformation due to EBK's sensitivity to outliers. Standard circular search neighborhood search parameters were used with a K-Bessel semivariogram model, allowing for the most accurate results. Using this tool allowed us to visualize the distribution of Hg contamination and identify Hg emission hotspots at the Sulphur Bank Mercury Mine.

3. Results

3.1 Transplantation Experiment

3.1.1 THg Accumulation

Linear regression and ANOVA tests revealed significant differences in the rates of mercury uptake among various lichen species, with notable variations depending on species and location. Linear regression tests were used to determine the rate constant of mercury uptake per day in the transplanted lichen. We found that each lichen species in the mercury uptake bags at the NAMD demonstrated an increase in THg concentrations over time. The only exception was the *Usnea* species located at shield 5, showing a decreasing slope of -0.0008082 per day, as

demonstrated in Table 1. The lichen species *Ramalina leptocarpha* demonstrated the largest increase in mercury concentration per day, as compared to *Usnea* and *Evernia*, in every shield except for shield 2. Linear regression revealed a significant relationship between the *Ramalina* lichen's exposure time and the rate constant of mercury accumulation in shields 1, 3, 4, and 5 (Table 1). An ANOVA test was performed to determine if the rate of mercury accumulation per day differed significantly between each lichen species. The ANOVA test revealed a significant difference in the rate of mercury accumulation per day among the three lichen species (Table 1) (ANOVA, $F(2,15) = 6.23$, $p = 0.0107$). A post-hoc Tukey test was then conducted given the statistically significant results of the ANOVA test, revealing that the rate of mercury accumulation per day is significantly smaller in *Usnea* than in *Ramalina leptocarpha* ($p = 0.008$), but no other pairs have significant differences. Out of all of the transplantation sites, shields 7,8, and 9 located in the Hacienda/Deep Gulch area, demonstrated the largest increase in THg per day. Linear regression tests revealed the transplanted lichen's exposure duration significantly influences the ratio between the lichen mercury concentrations at each time (q_L) and its initial mercury concentration (q^0_L), which increases as exposure increases in shields 7-9 (Table 1).

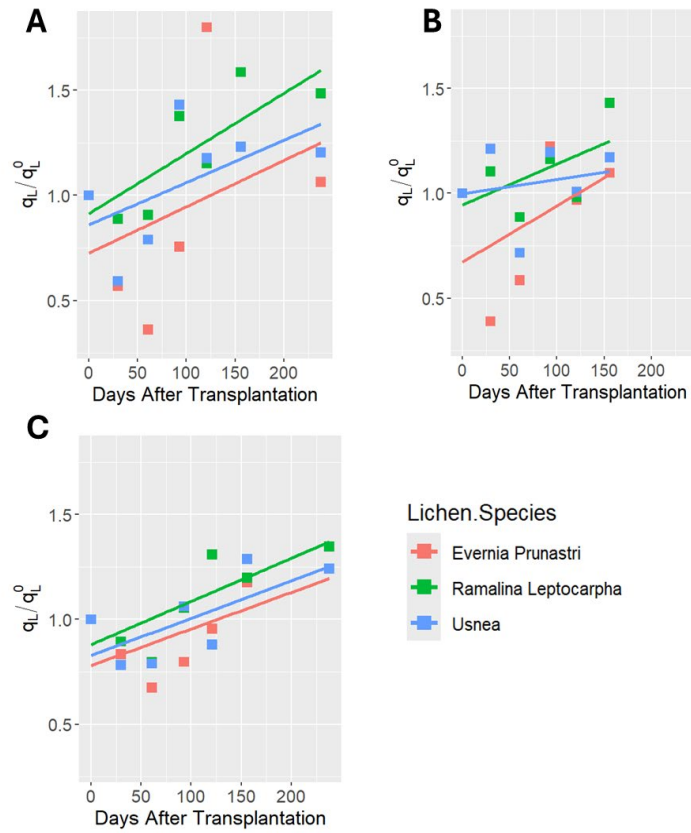


Figure 7: Plots of THg kinetic curves for lichen transplants 1-3 at the Mine Hill site color-coded by lichen species. Figure 7A represents shield 1 at Mine Hill, figure 7B represents shield 2 at Mine Hill, and figure 7C represents shield 3 at Mine Hill. Linear regression statistics are given in Table 1.

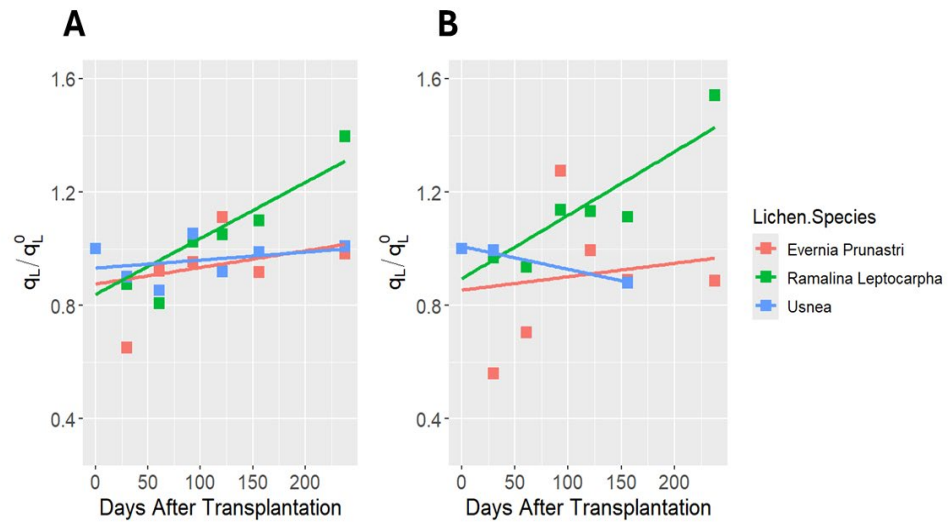


Figure 8: Plots of THg kinetic curves for lichen transplants 4 and 5 at the Almadén Reservoir site color-coded by lichen species. Figure 8A represents shield 4 at Almadén Reservoir and figure 8B represents Shield 5 at Almadén Reservoir. Linear regression statistics are given in Table 1.

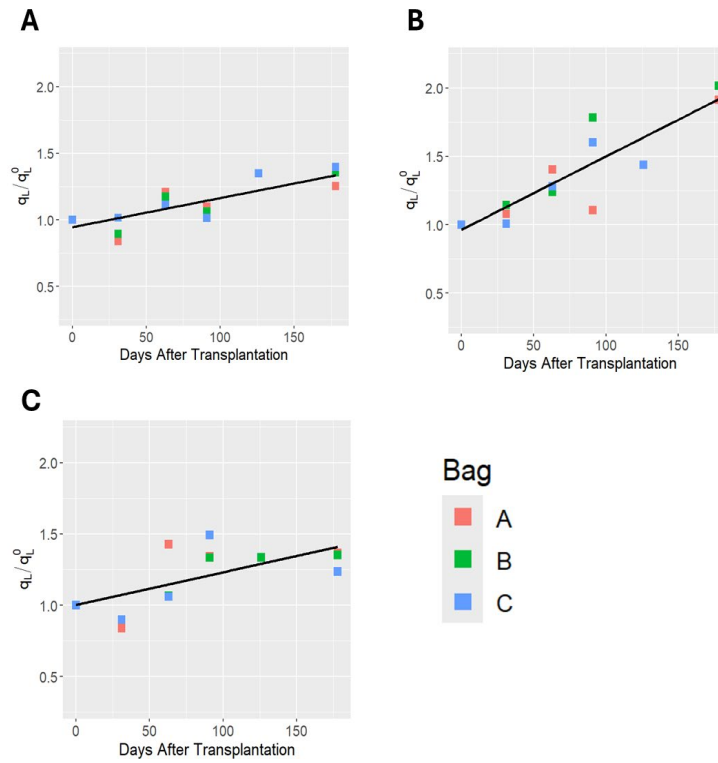


Figure 9: Plots of THg kinetic curves for lichen transplants 7-9 at the Hacienda site color-coded by mesh bags A, B, and C. Figure 9A represents shield 7, figure 9B represents shield 8, and figure 8C represents shield 9. Linear regression statistics are given in Table 1.

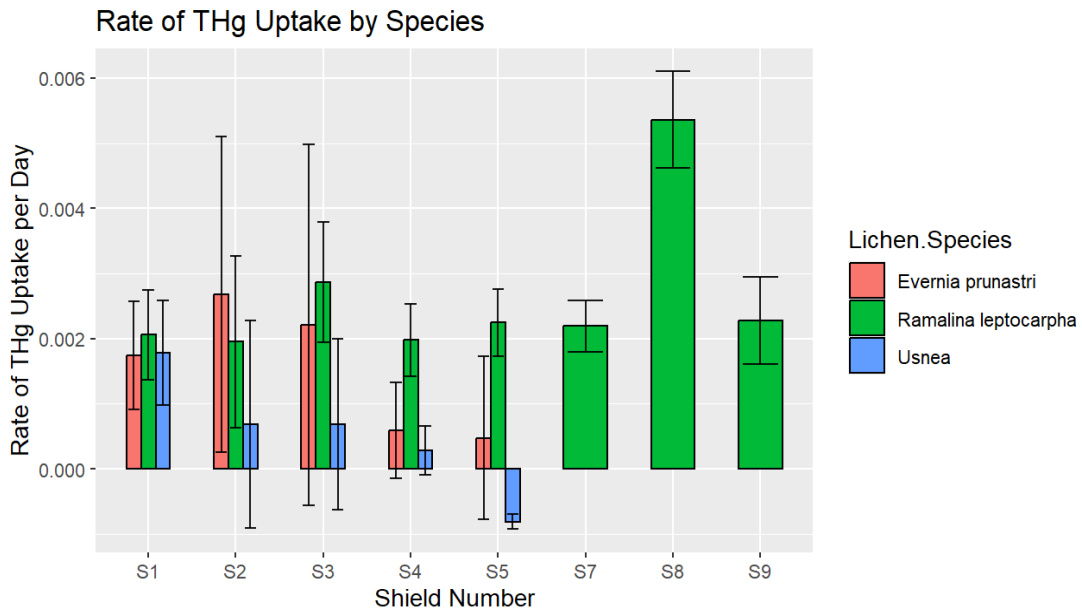


Figure 10: Bar plot demonstrating the slope of THg uptake per day for all lichen transplant shields at NAMD color-coded by lichen species *Evernia prunastri*, *Ramalina leptocarpha* and *Usnea sp.*. Shields 7-9 contained only *Ramalina leptocarpha*. The rates of THg uptake per day are given in Table 1.

Table 1: Linear regression statistics for shields 1-10. The slope describes the change in the rate of mercury accumulation and release per individual day.

Transplant Number	Transplant Type	Lichen Origin	Transplant Location	Lichen Species	Duration days	Slope	P-value	Standard Error
1	Uptake	Lexington	Mine Hill	<i>Ramalina leptocarpha</i>	238	0.002058	0.0312	0.0006932
1	Uptake	Lexington	Mine Hill	<i>Usnea</i>	238	0.001787	0.07683	0.0008038
1	Uptake	Lexington	Mine Hill	<i>Evernia prunastri</i>	238	0.001741	0.0886	0.000825
1	Control	Mine Hill	Mine Hill	<i>Evernia prunastri</i>	156	-0.000684	0.5029	0.0009008
2	Uptake	Lexington	Mine Hill	<i>Ramalina leptocarpha</i>	156	0.001951	0.2137	0.001321
2	Uptake	Lexington	Mine Hill	<i>Usnea</i>	156	0.000685	0.6883	0.0015877
2	Uptake	Lexington	Mine Hill	<i>Evernia prunastri</i>	156	0.00268	0.3301	0.002419
2	Control	Mine Hill	Mine Hill	<i>Usnea</i>	156	0.000304	0.8077	0.0011689
3	Uptake	Lexington	Mine Hill	<i>Ramalina leptocarpha</i>	238	0.002864	0.02673	0.0009227
3	Uptake	Lexington	Mine Hill	<i>Usnea</i>	238	0.000685	0.6883	0.001314
3	Uptake	Lexington	Mine Hill	<i>Evernia prunastri</i>	238	0.002206	0.4707	0.002772
3	Control	Mine Hill	Mine Hill	<i>Evernia prunastri</i>	156	0.000473	0.7522	0.0013982
4	Uptake	Lexington	Almaden	<i>Ramalina leptocarpha</i>	238	0.001979	0.01614	0.0005553
4	Uptake	Lexington	Almaden	<i>Usnea</i>	238	0.000282	0.4811	0.0003707
4	Uptake	Lexington	Almaden	<i>Evernia prunastri</i>	238	0.00059	0.4578	0.0007340
4	Control	Almaden	Almaden	<i>Evernia prunastri</i>	238	0.000406	0.6236	0.0007645
5	Uptake	Lexington	Almaden	<i>Ramalina leptocarpha</i>	238	0.002244	0.007639	0.0005205
5	Uptake	Lexington	Almaden	<i>Usnea</i>	156	-0.000808	0.09272	0.0001186
5	Uptake	Lexington	Almaden	<i>Evernia prunastri</i>	156	0.000475	0.7194	0.001249
5	Control	Almaden	Almaden	<i>Evernia prunastri</i>	238	0.000297	0.7283	0.0008088
6	Release	Mine Hill	Lexington	<i>Evernia prunastri</i>	208	0.004141	0.007526	0.0008293
6	Release	Mine Hill	Lexington	<i>Usnea</i>	208	0.003403	0.1274	0.001863
6	Release	Mine Hill	Lexington	<i>Evernia prunastri</i>	208	0.005686	0.3605	0.005281
6	Control	Lexington	Lexington	<i>Evernia prunastri</i>	208	5.40E-05	0.9378	6.497e-04
7	Uptake	Lexington	Deep Gulch	<i>Ramalina leptocarpha</i>	178	0.002191	7.94E-05	0.0003989
7	Control	Deep Gulch	Deep Gulch	<i>Ramalina leptocarpha</i>	126	0.001345	0.5237	0.001868
8	Uptake	Lexington	Hacienda	<i>Ramalina leptocarpha</i>	126	0.005358	6.89E-06	0.0007436
8	Control	Hacienda	Hacienda	<i>Ramalina leptocarpha</i>	126	-0.000196	0.9279	0.0019969
9	Uptake	Lexington	Hacienda	<i>Ramalina leptocarpha</i>	178	0.002278	0.004683	0.0006688
9	Control	Hacienda	Hacienda	<i>Evernia prunastri</i>	178	0.000557	0.85	0.0005565
10	Release	Hacienda	Lexington	<i>Ramalina leptocarpha</i>	178	-0.000185	0.8821	0.0011720
10	Release	Hacienda	Lexington	<i>Evernia prunastri</i>	126	-0.002143	0.1519	0.001121
10	Control	Lexington	Lexington	<i>Ramalina leptocarpha</i>	178	0.001306	0.2095	0.0008743

3.1.2 THg Release

To measure the rate of Hg release in lichens, we transplanted native lichens from the NAMD to the Lexington Reservoir. Lichens were collected at various locations with known elevated Hg concentrations, including Mine Hill, Deep Gulch, and the Hacienda Furnace Yard.

They were then transplanted to the same location at the Lexington Reservoir, suspended from shields 6 and 10. Shield 6 included only *Evernia prunastri* and *Usnea*, while shield 10 included *Evernia prunastri* and *Ramalina leptocarpha*. Shield 6, with lichen originating from Mine Hill, did not show a decreasing trend in mercury release and revealed a positive rate of mercury uptake over time. Linear regression tests showed a significant relationship between the lichen's exposure time and the rates of mercury accumulation in the *Evernia prunastri* species at shield 6 (Table 1). It is important to note that the location of shield 6 at the Lexington reservoir was not a source of Hg contamination, as the control bag did not demonstrate an increase in Hg concentration over time. Linear regression tests did not reveal any statistically significant relationships between the exposure duration of lichens and the rates of mercury accumulation and release in the other lichen species at shields 6 and 10. At shield 10, with lichen originating from the Hacienda/Deep Gulch area, a sharp decline in THg was observed in the *Evernia prunastri* species, contrasting with a variable release of THg in *Ramalina leptocarpha* over time.

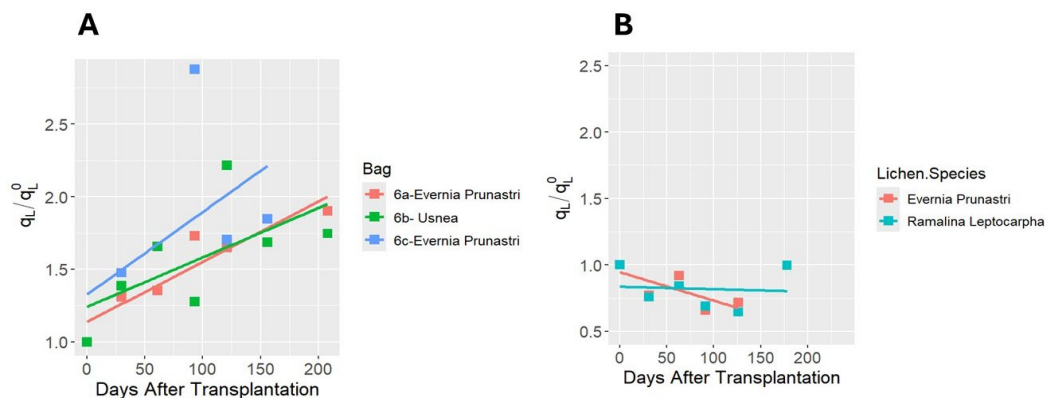


Figure 11: Plots of THg kinetic curves for lichen transplants 6 and 10 at the Lexington Reservoir color-coded by lichen species. Figure 11A represents shield 6 at Lexington Reservoir with lichen originating from Mine Hill. Figure 11B represents shield 10 at Lexington Reservoir with lichen originating from the Hacienda area. Linear regression statistics are given in Table 1.

3.1.3 THg in Controls

In addition to the three bags that contained transplanted lichen, control bags were suspended from each shield. The control bags consisted of native lichens gathered from each respective shield location. A steady increase in the rate of THg uptake was observed in most of the shields. The only exceptions to this were *Evernia Prunastri* at Shield 1, collected and suspended at Mine Hill, and *Ramalina leptocarpha* at Shield 8, collected and suspended at the Hacienda furnace yard. The controls at shields 1 and 8 demonstrated negative slopes in THg accumulation per day (Table 1). No significant trends were observed in the controls at shields 6 and 10 at the Lexington reservoir. Linear regression tests determined no statistically significant

relationships between the exposure duration of lichens and the rates of mercury accumulation and release in the control species at each shield ($p=0.05$) (Table 1).

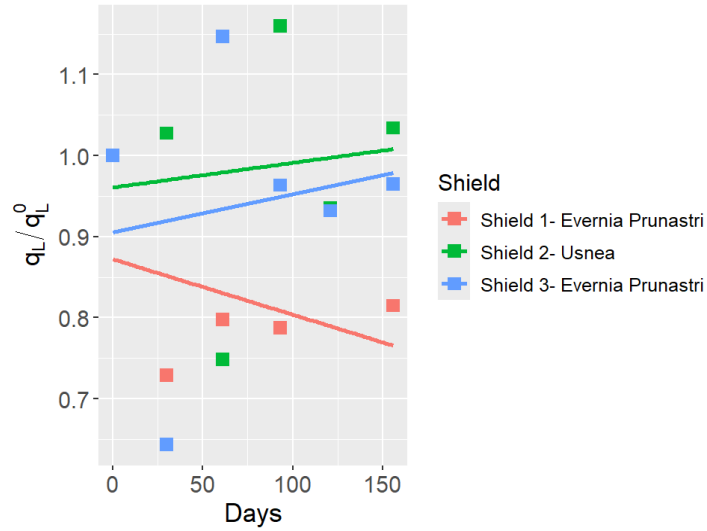


Figure 12: Plots of THg kinetic curves for lichen controls CS1, CS2, and CS3 at the Mine Hill site color-coded by shield. Linear regression statistics are given in Table 1.

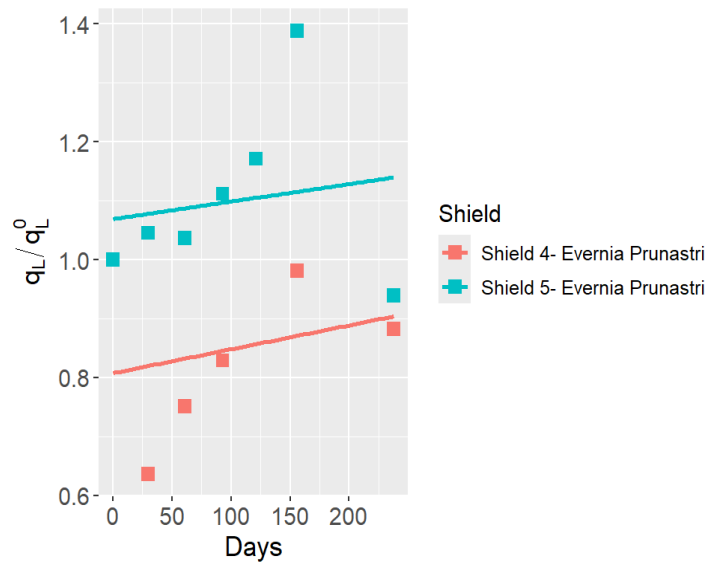


Figure 13: Plots of THg kinetic curves for lichen controls CS4 and CS5 at the Almadén Reservoir site color-coded by shield. Linear regression statistics are given in Table 1.

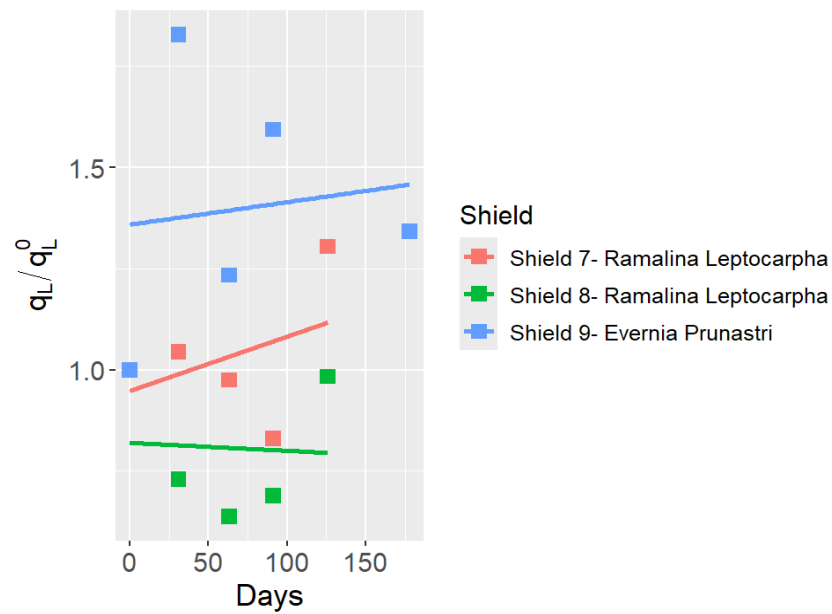


Figure 14: Plots of THg kinetic curves for lichen controls CS7, CS8, and CS9 at the Hacienda/Deep Gulch sites color-coded by shield. Linear regressions statistics are given in Table 1.

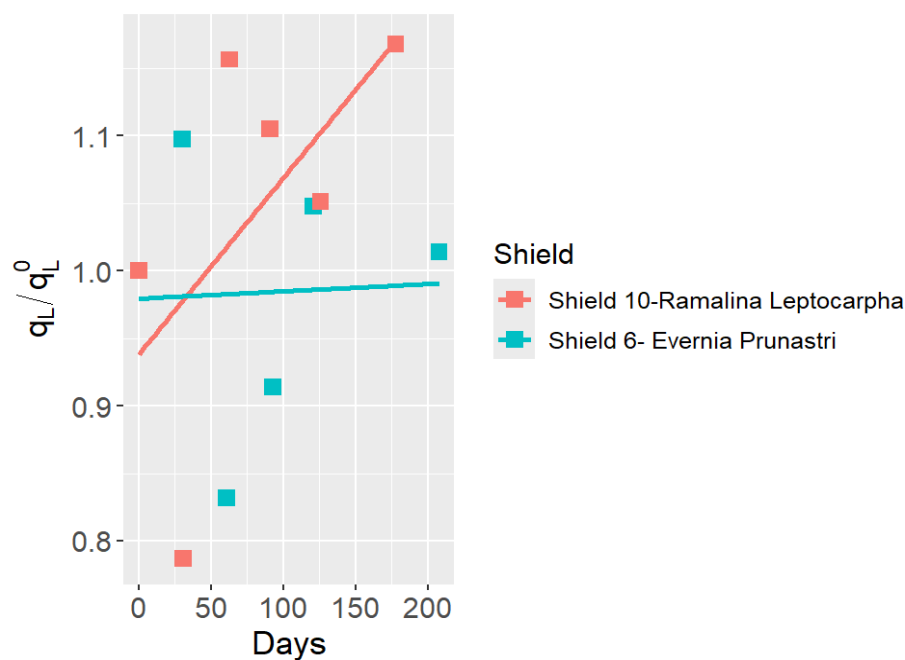


Figure 15: Plots of THg kinetic curves for lichen controls CS6 and CS10 at the Lexington Reservoir site color-coded by shield. Linear regressions statistics are given in Table 1.

3.1.4 MerPAS Results

After analysis, MerPAS results indicated the average elemental mercury concentration in nanograms per cubic meter of air sampled for each shield location (Table 2). Gaseous Hg concentrations in the MerPAS ranged from 0.845-2.02 ng/m³ (Table 2). The lowest concentration of 0.845 ng/m³ was recorded at the Lexington Reservoir near shield 6. The highest concentration of 2.02 ng/m³ was recorded at the Hacienda Furnace Yard near shield 8, corresponding with the elevated rates of THg uptake observed in the transplanted lichen. The four locations including Mine Hill, Lexington Reservoir, Almaden Reservoir, and the Hacienda/Deep Gulch area showed distinctly different air concentrations. An atmospheric mercury monitoring study

conducted by Gačnik et al compared active measurements, lichen biomonitoring, and passive sampling to assess atmospheric Hg concentrations at the Idrija Mercury Mine in Idrija, Slovenia⁵². This study deployed multiple MerPAS for a 12-week period using a sampling rate of $0.131 \text{ m}^3 \text{ day}^{-1}$, finding average Hg^0 concentrations of 13-17 ng/m^3 around a historical Hg smelting area at the Idrija mine⁵². They also deployed MerPAS for a 12-week period in the town of Anhova that is known for elevated Hg concentrations due to cement production, resulting in average Hg^0 concentrations of 1.6-1.7 ng/m^3 ⁵². Compared to this study, our concentrations of 2.02 ng/m^3 recorded at the Hacienda Furnace Yard are relatively low for Hg monitoring at an abandoned mercury mine, suggesting that NAMD is not as contaminated as other Hg mines including the Idrija Mercury Mine. The sampling rate we selected was $0.111 \text{ m}^3 \text{ day}^{-1}$ as recommended by the Tekran Corporation^{46,47}. In the future, it may be more appropriate to use a higher sampling rate as shown by Gačnik et al⁵².

The data from the MerPAS was normally distributed, and a Pearson's linear correlation test was used to determine a correlation between the concentration of Hg^0 as indicated by the MerPAS and the slopes of THg accumulation per day of *Ramalina* lichen in transplants 1-5, 7-9, and the control lichen from shield 6. Pearson's linear correlation test revealed a significant positive correlation between the lichen's daily rate of THg accumulation and the average elemental mercury concentration in the MerPAS (Pearson's correlation: $r = 0.73$, $p = 0.02$). A positive correlation implies that the rates of THg accumulation in the transplanted lichens are proportional to the

MerPAS concentrations for each shield location, indicating that the transplanted lichens are reacting to their altered atmospheric conditions.

Table 2: A table summarizing the average elemental mercury concentrations in the MerPAS at Shields 1-9.

Transplant Number	Location	Duration Days	N (Samples)	Mean Air Hg Concentration (ng/m3)	Range of Air Hg Concentration (ng/m3)
1	Mine Hill	60.9	2	1.30	0.177
2	Mine Hill	61	2	1.50	0.145
3	Mine Hill	60.9	2	1.41	0.0475
4	Almaden Reservoir	61	2	0.938	0.0926
5	Almaden Reservoir	60.1	2	1.38	0.768
6	Lexington	61	2	0.845	0.105
7	Deep Gulch	62.9	2	1.92	0.0372
8	Hacienda	59.9	2	2.02	0.644
9	Hacienda	62.9	2	1.78	0.431

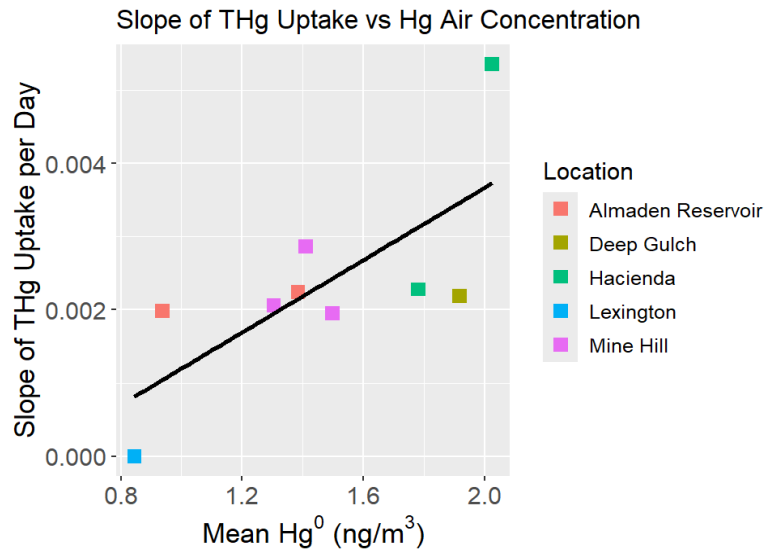


Figure 16: A scatterplot illustrating the relationship between the daily rates of THg accumulation in transplanted lichens and average elemental mercury concentrations in the MerPAS, color-coded by shield location. Each data point represents a specific measurement taken at shield locations 1-9.

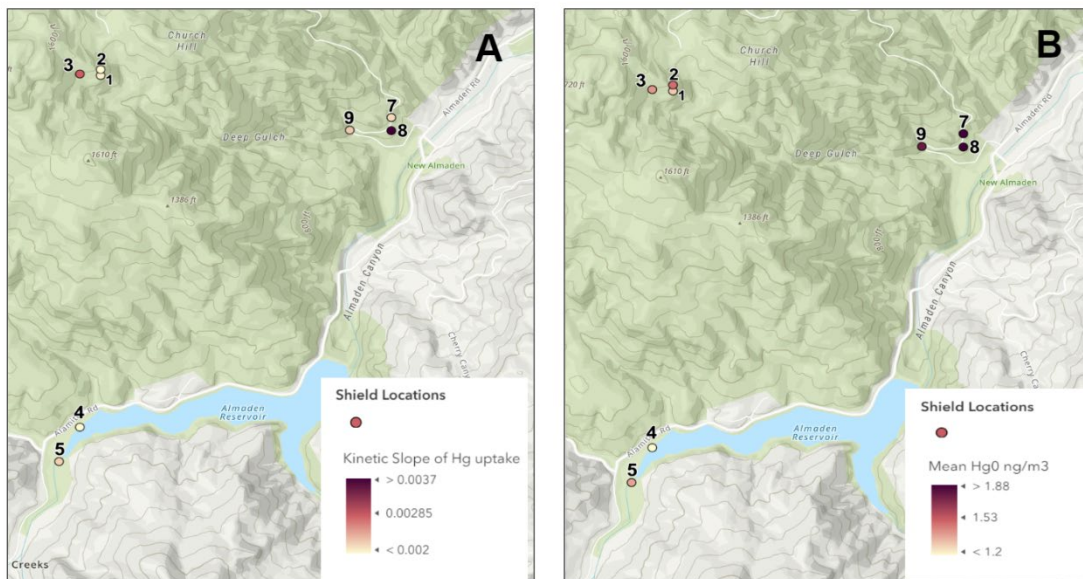


Figure 17: Figure 17A shows a map illustrating the spatial distribution of daily rates of THg accumulation in shields 1-9. Figure 17B depicts a map illustrating the spatial distribution of average atmospheric elemental mercury (Hg⁰) concentrations from the MerPAS, in shields 1-9.

3.2 Sulphur Bank Mercury Mine

3.2.1 Total Mercury Concentrations in Lichens within SBMM and the Surrounding Areas

Throughout the SBMM area, mean THg concentrations within lichen ranged from 299 to 45,348 ppb. Lichen samples collected at the Tailings pile, the South Waste Rock Pile, and the West Waste Rock Pile south of the Herman Impoundment demonstrated the highest mean total mercury concentrations, ranging from 11,025 to 45,348 ppb. These findings imply that these locations serve as significant Hg emission hotspots. The application of ArcGIS Pro's Empirical Bayesian Kriging analysis tool validated the identification of hotspots at SBMM through data

interpolation techniques to create reliable spatial predictions (Figure 18). This method considers the variability in the data, enhancing the confidence in the identified hotspots through statistical validation⁵¹. The tailings pile south of the Herman Impoundment was once used as a calcine processing site, revealing the highest mean THg concentration among our lichen samples, peaking at 45,348 ppb. This area previously hosted a furnace plant in 1931, directly aligning with the site of the lichen sampled exhibiting this elevated THg concentration. These results demonstrate how lichen can be used as an effective bioindicator of atmospheric mercury emissions at mining sites.

Lichen sampled at the Satellite Waste rock pile and the North Waste rock pile located north of the Herman Impoundment revealed relatively lower mean THg concentrations, ranging from 299 to 6,663 ppb. Our results indicated that mean THg concentrations within lichens decreased with distance from known hotspots of atmospheric Hg emissions, particularly those once used as calcine processing areas.

We collected additional lichen samples from background locations to serve as control specimens. Background sites included the Ukiah Airport, Nice, Cole Creek, Middle Creek, and Kelsey Creek, located northwest of the Herman Impoundment. Mean THg concentrations in control samples from these background sites ranged from 140 to 939 ppb. The highest THg concentration of 939 ppb was observed in Nice, approximately 29 km north of the SBMM. The lowest concentration of 140 ppb was sampled from Kelsey Creek, approximately 15 km west of the SBMM. These

results suggest that other sources of Hg may exist considerably beyond the mine's vicinity, such as enriched soils in naturally occurring mercury deposits⁵³.

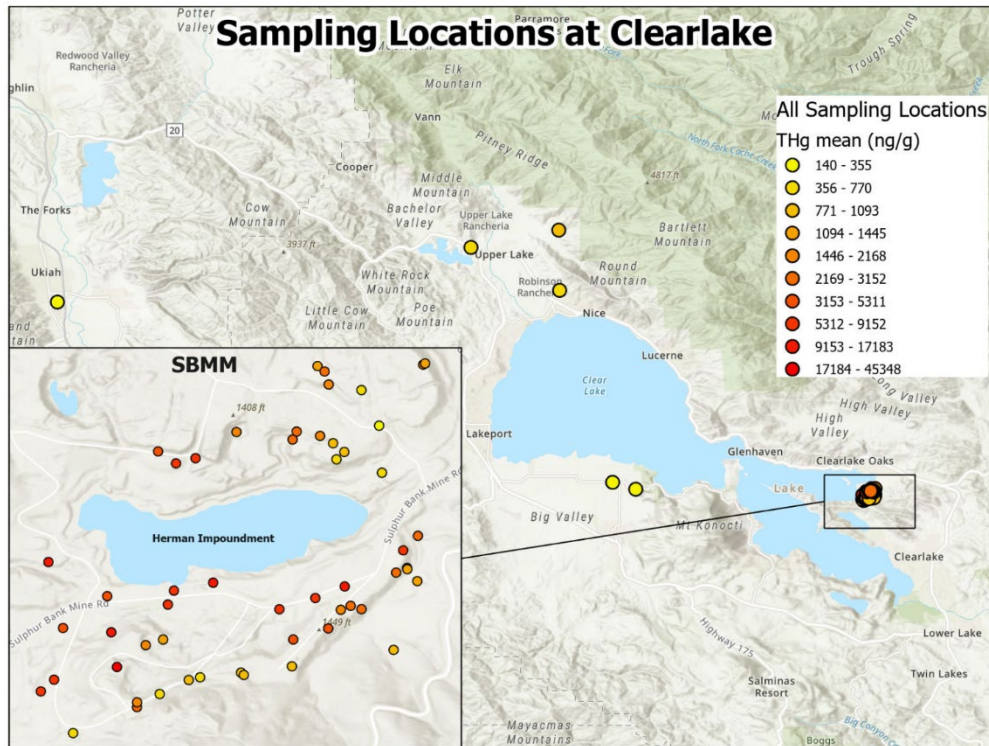


Figure 18: Map demonstrating the sampling locations at SBMM and surrounding areas in the Clearlake region. Each point represents a sampling location of lichen with a corresponding THg concentration. All points outside of the SBMM represent control samples at background locations.

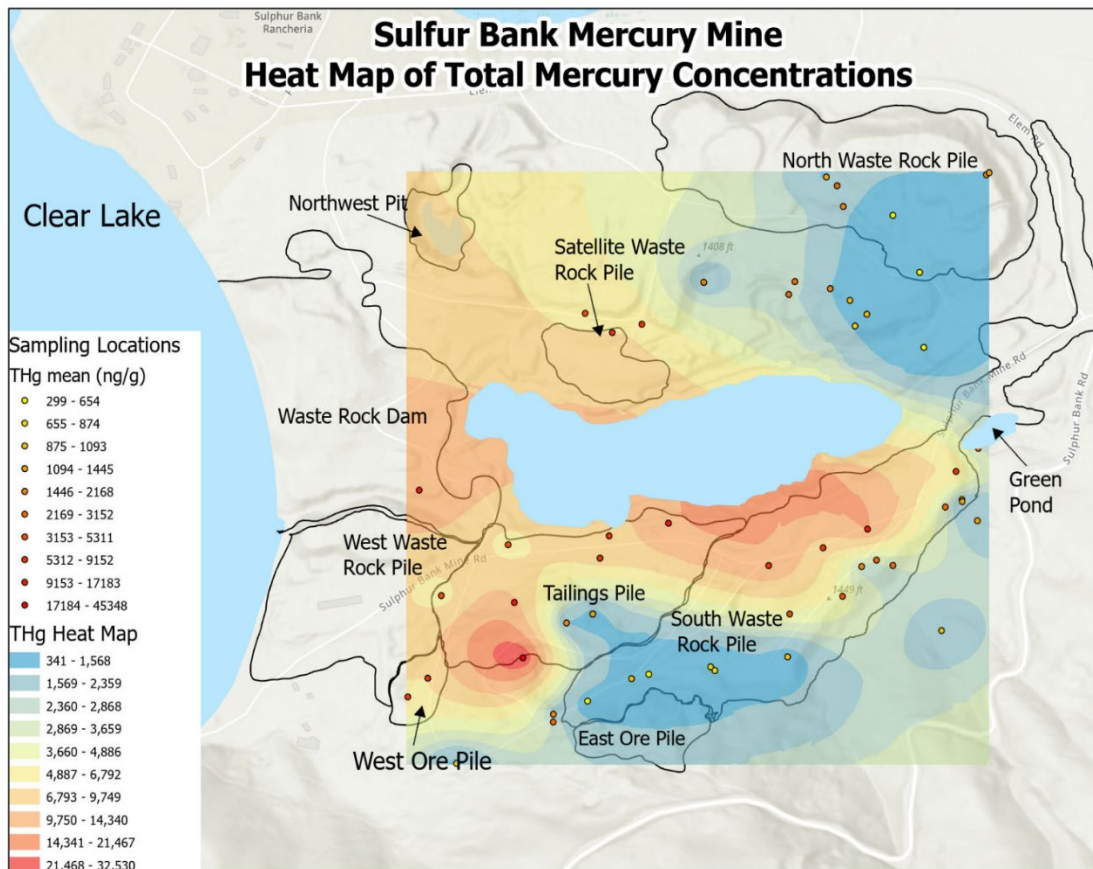


Figure 19: Heat map of total mercury concentrations at the SBMM, with notable mine waste piles labeled. This map was made using ArcGIS's Empirical Bayesian Kriging analysis tool. Each point represents a sampling location of lichen with a corresponding THg concentration.

3.2.2 Total Mercury Concentration by Lichen Species

Multiple lichen species were sampled at SBMM to explore potential differences in sensitivity to total mercury depending on species and morphological characteristics. Our lichen sampling at SBMM was divided into multiple lichen collection zones with species sampled at the south waste rock pile and the Green Pond southeast of the Herman Impoundment, the tailings pile and the south waste

rock pile south of the Herman Impoundment, the Satellite waste pile and disturbed rock north of the Herman Impoundment, and the North-Waste rock pile. Within each lichen collection zone, we took various samples of lichen and then separated those samples by species at the laboratory. Based on their abundance in the area and ease of visual identification, the lichen species *Evernia prunastri*, *Ramalina leptocarpha*, *Usnea sp.*, *Ramalina Farinacea*, and *Ramalina menziesii* were sampled. We observed variability in the mean THg concentrations among the various lichen species. The data was determined to be non-normally distributed, and a Kruskal-Wallice test was performed to evaluate potential variations in mean THg concentrations among sampled species, revealing no statistically significant differences ($H = 8.68$, $df = 4$, $p = 0.07$). These findings suggest that the choice of species is unlikely to significantly impact the identification of areas with heightened mercury emissions when using lichen as a bioindicator.

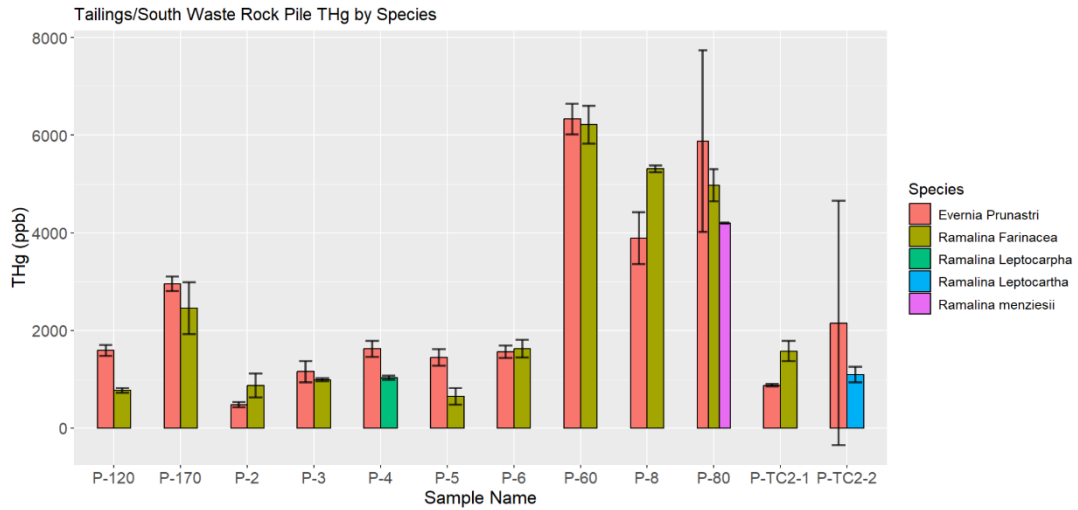


Figure 20: Bar graph comparing the mean THg concentrations of lichen samples, color-coded by species. These samples were collected from the tailings pile and the south waste rock pile south of the Herman Impoundment.

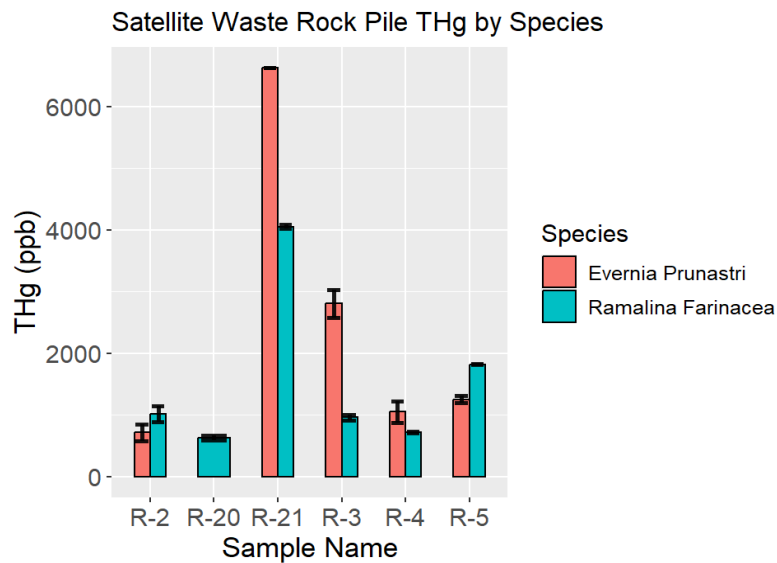


Figure 21: Bar graph comparing the mean THg concentrations of lichen samples, color-coded by species. These samples were collected from the Satellite waste pile and disturbed rock north of the Herman Impoundment.

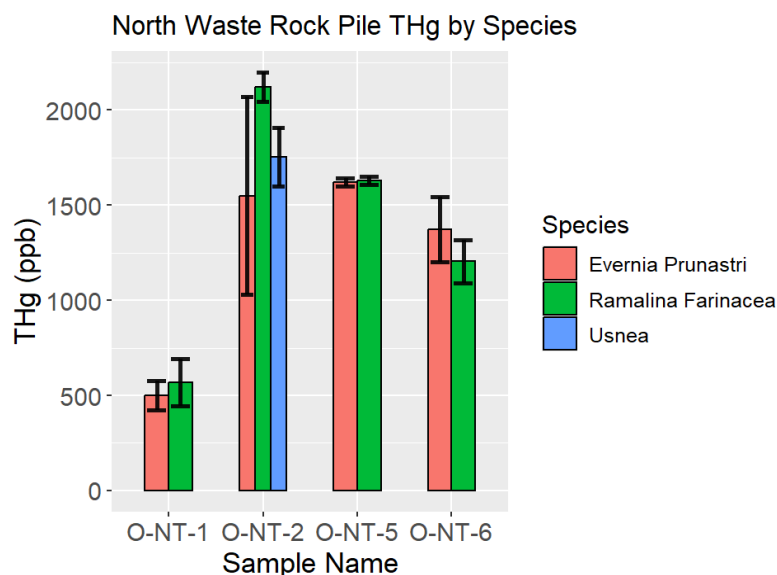


Figure 22: Bar graph comparing the mean THg concentrations of lichen samples color-coded by species. These samples were collected from the North-Waste rock pile north of the Herman Impoundment.

4. Discussion

4.1 Lichen as a Bioindicator

Lichens can serve as an inexpensive and effective technique for the active biomonitoring of atmospheric mercury in a contaminated environment. In this study, we accomplished our objectives of identifying Hg emissions and deposition at the NAMD and SBMM by utilizing lichen as a bioindicator. Our study investigated the dynamics of THg accumulation in lichens across different species and contaminated settings, aiming to elucidate the rate of uptake of Hg in lichen.

4.2 THg Accumulation and Release by Transplanted Lichens at NAMD

4.2.1 Effect of Lichen Species on THg Accumulation

In our transplantation experiment at the NAMD, results indicated that species played a significant role in THg accumulation within transplanted lichens. Linear regression tests revealed statistically significant relationships between the *Ramalina* lichen's exposure time and the rates of mercury accumulation in every uptake shield except for shield 2 (Table 1). Compared to *Usnea sp.* and *Evernia prunastri*, the *Ramalina* species demonstrated the largest daily rate of THg accumulation in every shield except for shield 2 (Table 1). Numerous studies have reported that the age and extent of surface area in lichen species can impact the accumulation of heavy metals^{31,37,39}. The lichen species selected for our study were epiphytic fruticose lichens with varying surface area, possibly resulting in an unequal accumulation of Hg.

4.2.2 Hg Emission Hotspots at NAMD

In addition to lichen species, our results highlighted the significant influence of transplantation sites on the rates of THg accumulation in lichens. Linear regression tests revealed statistically significant relationships between the transplanted lichen's exposure time and the rates of mercury accumulation in shields 7-9, all located in the Hacienda/Deep Gulch area (Table 1). Transplanted lichens in the Hacienda/Deep Gulch area showed the largest increase in the rates of THg accumulation out of all of the transplant sites. These results indicate that the Hacienda/Deep Gulch areas at the NAMD are Hg emission hotspots. Historically, the Hacienda Furnace Yard was a calcine processing area where cinnabar ore was heated in a furnace to extract and

condense elemental mercury vapor²⁰. Large amounts of calcine deposits remain in the Hacienda and Deep Gulch area, even with remediation efforts in place²⁰. The rates of THg accumulation in the transplanted lichens reveal that calcines and mercury-contaminated soils at these locations continue to represent significant sources of Hg emissions. It thus supports our overall objective in identifying Hg emission hotspots and pathways of contamination by using lichen as a bioindicator.

4.2.3 THg Release

Our results demonstrated variability in the rates of THg release within lichens transplanted from the Hacienda/Deep Gulch area to the Lexington reservoir. Shield 6, with lichen originating from Mine Hill, revealed a positive rate of mercury uptake over time instead of the decreasing trend we were expecting. The *Ramalina* species at Shield 10 first demonstrated a decreasing trend in the rate of THg release, but then spiked in THg concentration during the last time point. These variable results can possibly be explained by our method of sampling and analysis. As we subsampled the lichen transplants, we collected different parts of the lichen and then crushed them together. When analyzing the subsamples in the DMA, we then scooped out a small portion of the dried lichen subsamples. As stated previously, the fruticose lichen involved in this study possibly have an unequal accumulation of Hg due to the varying surface area of each species. Additionally, numerous studies have shown that the age of the thallus can influence heavy metal accumulation, with older, inner areas of the lichen demonstrating higher concentrations of heavy metals compared to

peripheral areas^{37,39}. These factors might explain how our method in sampling and analyzing different parts of the lichen may have resulted in variable THg concentrations over time. In the future it would be good to normalize the accumulation to surface area and age. Another possible explanation for our results of the lichens transplanted to the Lexington reservoir might be due to the length of time the lichens stayed in the field. A transplantation study conducted by Vannini et al (2021) found that transplanted lichens accumulated mercury proportionally to the incubation concentrations and then released mercury over time. The results in the Vannini et al experiment showed that the lichens eventually decreased to stable concentrations after 6-24 months⁴¹. The lichens involved in our experiment were only transplanted to the Lexington reservoir for 7 months, and this may have not been enough time for them to release THg and eventually reach stable concentrations that reflect the environmental setting.

4.3 Hg Pathways at SBMM

Our investigation at the SBMM revealed no statistically significant differences in THg concentrations among the various lichen species sampled. Although our results at SBMM suggested that the choice of lichen species may not significantly impact the identification of atmospheric mercury emission hotspots, our results at NAMD indicated a species-specific response to THg accumulation. Utilizing lichen as a bioindicator at the SBMM allowed us to pinpoint areas of elevated atmospheric mercury emissions, as high THg concentrations in lichens

correlate with the historical land usage. The tailings pile south of the Herman Impoundment exhibited the highest THg concentration found within our lichen samples. This location was formerly the main calcine processing area of the SBMM, once the site of condenser plants where extracted mercury was condensed into elemental mercury vapor, retort and rotary furnace plants used to heat cinnabar, screening and sorting plants, and mud overflow ponds used to store calcines. South of the condenser plant remains a large calcine dump in the tailings pile. Elevated THg concentrations at this location demonstrate that this area continues to remain a significant hotspot of atmospheric mercury emissions and deposition in comparison to the other mine waste piles. Regardless as previous studies reported species dependence of THg uptake although our data does not show this dependence we advise that future studies should use a single species for comparison to reduce species dependence effects.

5. Conclusions

5.1 Impact of Research

Our research involving lichen as bioindicators shed light on mercury emissions and transport dynamics at the NAMD and the SBMM. Furthermore, our findings can inform future studies utilizing lichen as bioindicators for atmospheric mercury in contaminated environments. By providing valuable insights into Hg distribution and emission hotspots, this research can assist state and government agencies in remediation efforts and inform future policy decisions. Identifying

hotspots of atmospheric mercury emissions and deposition is crucial for mitigating the adverse effects of mercury on ecosystems and human health. The ability of lichens to reflect historical land usage patterns, as demonstrated through our research, illustrates their use as sensitive bioindicators of environmental change over time. In addition to contributing to the understanding of mercury cycling in contaminated settings, our research offers guidance in biomonitoring strategies aimed at reducing mercury pollution.

5.2 Future Studies

While our research has provided valuable information regarding the use of lichen as bioindicators of atmospheric mercury, future studies are necessary to increase our understanding of the complex dynamics of Hg transport in a contaminated environment. The extreme winter weather of 2023 most likely impacted the Hg concentrations in lichen at NAMD, as low temperatures likely lowered Hg emission rates from contaminated soil. The anomalous weather patterns in 2023 likely compromised our experiment at NAMD, revealed by the variability in the rates of THg accumulation and release over the winter months. In August of 2023, we decided to start a new transplantation experiment for shields 7-9 in the Mine Hill/Hacienda area. We chose these locations as lichens transplanted to the Mine Hill/Hacienda areas showed the largest THg increase over time out of all of the shields in the first transplantation experiment. Beginning a new transplantation study will allow us to determine the Hg uptake rates in transplanted lichens throughout the

dryer and warmer months. This study will continue until June of 2024 and the lichen samples at the last time point will be analyzed for THg and Hg isotope ratios.

Furthermore, we aim to analyze the mercury isotopes and speciated form of mercury within the lichens at the SBMM. Examining the speciated form of mercury within the lichens will provide valuable information regarding potential mercury mobilization, methylation, and remission into the atmosphere. This analysis will allow us to distinguish between natural and anthropogenic sources of Hg emissions, as well as provide a better understanding into the pathway of Hg contamination at SBMM. Additionally, analyzing mercury isotopes within our lichen samples will enhance the Hg isotope data currently compiled by the USGS. These results will play a crucial role in determining the impacts of mine waste on Hg bioaccumulation within the Clear Lake food web.

6. Bibliography

1. Selin, N. E. Global Biogeochemical Cycling of Mercury: A Review. *Annual Review of Environment and Resources*, 2009, 34, 43–63.
<https://doi.org/10.1146/annurev.environ.051308.084314>.
2. Kolipinski, M.; Subramanian, M.; Kristen, K.; Borish, S.; Ditta, S. Sources and Toxicity of Mercury in the San Francisco Bay Area, Spanning California and Beyond. *J Environ Public Health* 2020, 2020, 8184614.
<https://doi.org/10.1155/2020/8184614>.
3. Kim, M.-K.; Zoh, K.-D. Fate and Transport of Mercury in Environmental Media and Human Exposure. *J Prev Med Public Health* 2012, 45 (6), 335–343. <https://doi.org/10.3961/jpmph.2012.45.6.335>.
4. Schiavo, B.; Morton-Bermea, O.; Salgado-Martínez, E.; García-Martínez, R.; Hernández-Álvarez, E. Health Risk Assessment of Gaseous Elemental Mercury (GEM) in Mexico City. *Environ Monit Assess* 2022, 194 (7), 456.
<https://doi.org/10.1007/s10661-022-10107-7>.
5. Pirrone, N.; Cinnirella, S.; Feng, X.; Finkelman, R. B.; Friedli, H. R.; Leaner, J.; Mason, R.; Mukherjee, A. B.; Stracher, G. B.; Streets, D. G.; Telmer, K. Global Mercury Emissions to the Atmosphere from Anthropogenic and Natural Sources. *Atmospheric Chemistry and Physics* 2010, 10 (13), 5951–5964. <https://doi.org/10.5194/acp-10-5951-2010>.
6. Mason, R. P.; Fitzgerald, W. F.; Morel, F. M. M. The Biogeochemical Cycling of Elemental Mercury: Anthropogenic Influences. *Geochimica et*

- Cosmochimica Acta* 1994, 58 (15), 3191–3198. [https://doi.org/10.1016/0016-7037\(94\)90046-9](https://doi.org/10.1016/0016-7037(94)90046-9).
7. Rimondi, V.; Benesperi, R.; Beutel, M. W.; Chiarantini, L.; Costagliola, P.; Lattanzi, P.; Medas, D.; Morelli, G. Monitoring of Airborne Mercury: Comparison of Different Techniques in the Monte Amiata District, Southern Tuscany, Italy. *Int J Environ Res Public Health* 2020, 17 (7), 2353. <https://doi.org/10.3390/ijerph17072353>.
 8. *The Genetic Basis for Bacterial Mercury Methylation*. <https://doi.org/10.1126/science.1230667>.
 9. Qing, Y.; Li, Y.; Yang, J.; Li, S.; Gu, K.; Bao, Y.; Zhan, Y.; He, K.; Wang, X.; Li, Y. Risk Assessment of Mercury through Dietary Exposure in China. *Environmental Pollution* 2022, 312, 120026. <https://doi.org/10.1016/j.envpol.2022.120026>.
 10. US EPA, O. *Minamata Convention on Mercury*. <https://www.epa.gov/international-cooperation/minamata-convention-mercury> (accessed 2024-04-09).
 11. Stoffersen, B.; Appel, P. W.; Na-Oy, L. D.; Sekamane, A. S.; Ruiz, I. Z.; Køster-Rasmussen, R. Introduction of Mercury-Free Gold Extraction to Small-Scale Miners in the Cabo Delgado Province in Mozambique. *J Health Pollut* 2018, 8 (19), 180909. <https://doi.org/10.5696/2156-9614-8.19.180909>.

12. Alpers, C. N.; Hunerlach, M. P. *Mercury Contamination from Historic Gold Mining in California*; U.S. Department of the Interior, U.S. Geological Survey, 2000.
13. Gosar, M.; Teršič, T. Environmental Geochemistry Studies in the Area of Idrija Mercury Mine, Slovenia. *Environ Geochem Health* 2012, *34 Suppl 1*, 27–41. <https://doi.org/10.1007/s10653-011-9410-6>.
14. Eckley, C. S.; Gilmour, C. C.; Janssen, S.; Luxton, T. P.; Randall, P. M.; Whalin, L.; Austin, C. The Assessment and Remediation of Mercury Contaminated Sites: A Review of Current Approaches. *Sci Total Environ* 2020, *707*, 136031. <https://doi.org/10.1016/j.scitotenv.2019.136031>.
15. Kim, C. S.; Brown, G. E.; Rytuba, J. J. Characterization and Speciation of Mercury-Bearing Mine Wastes Using X-Ray Absorption Spectroscopy. *Sci Total Environ* 2000, *261* (1–3), 157–168. [https://doi.org/10.1016/s0048-9697\(00\)00640-9](https://doi.org/10.1016/s0048-9697(00)00640-9).
16. Rytuba, J. Mercury from Mineral Deposits and Potential Environmental Impact. *Environmental Geology* 2003, *43*, 326–338. <https://doi.org/10.1007/s00254-002-0629-5>.
17. Cargill, S. M.; Root, D. H.; Bailey, E. H. Resource Estimation from Historical Data: Mercury, a Test Case. *Mathematical Geology* 1980, *12* (5), 489–522. <https://doi.org/10.1007/BF01028882>.
18. Cox, M. The History of Mercury Emissions from the New Almaden Mines, Santa Clara County, California (2000, Edited 2011); 2000.

19. New Almaden Quicksilver Trustee Council. Decision document concerning the Almaden Quicksilver Restoration Plan and Environmental Assessment. Administrative Record. California Department of Fish and Game, Office of Spill Prevention and Response; 7/16/2007.
<https://nrm.dfg.ca.gov/FileHandler.ashx?DocumentID=17362>
20. *Hacienda and Deep Gulch Remediation Project - Parks and Recreation - County of Santa Clara*. <https://parks.sccgov.org/hacienda-and-deep-gulch-remediation-project> (accessed 2024-04-10).
21. Rytuba, J. J. Mercury Mine Drainage and Processes That Control Its Environmental Impact. *Science of The Total Environment* 2000, 260 (1), 57–71. [https://doi.org/10.1016/S0048-9697\(00\)00541-6](https://doi.org/10.1016/S0048-9697(00)00541-6).
22. López Berdonces, M. A.; Higuera, P. L.; Fernández-Pascual, M.; Borreguero, A. M.; Carmona, M. The Role of Native Lichens in the Biomonitoring of Gaseous Mercury at Contaminated Sites. *J Environ Manage* 2017, 186 (Pt 2), 207–213. <https://doi.org/10.1016/j.jenvman.2016.04.047>.
23. Jiménez-Moreno, M.; Barre, J. P. G.; Perrot, V.; Bérail, S.; Rodríguez Martín-Doimeadios, R. C.; Amouroux, D. Sources and Fate of Mercury Pollution in Almadén Mining District (Spain): Evidences from Mercury Isotopic Compositions in Sediments and Lichens. *Chemosphere* 2016, 147, 430–438. <https://doi.org/10.1016/j.chemosphere.2015.12.094>.

24. *SULPHUR BANK MERCURY MINE Site Profile*.
<https://cumulis.epa.gov/supercpad/SiteProfiles/index.cfm?fuseaction=second.Cleanup&id=0902228#bkground> (accessed 2024-04-11).
25. Suchanek, T. H.; Mullen, L. H.; Lamphere, B. A.; Richerson, P. J.; Woodmansee, C. E.; Slotton, D. G.; Harner, E. J.; Woodward, L. A. Redistribution of Mercury from Contaminated Lake Sediments of Clear Lake, California. *Water, Air, & Soil Pollution* 1998, *104* (1), 77–102.
<https://doi.org/10.1023/A:1004980026183>.
26. Gustin, S. M.; Coolbaugh, M.; Engle, M.; Fitzgerald, B.; Keislar, R.; Lindberg, S.; Nacht, D.; Quashnick, J.; Rytuba, J.; Sladek, C.; Zhang, H.; Zehner, R. Atmospheric Mercury Emissions from Mine Wastes and Surrounding Geologically Enriched Terrains. *Env Geol* 2003, *43* (3), 339–351. <https://doi.org/10.1007/s00254-002-0630-z>.
27. Fantozzi, L.; Ferrara, R.; Dini, F.; Tamburello, L.; Pirrone, N.; Sprovieri, F. Study on the Reduction of Atmospheric Mercury Emissions from Mine Waste Enriched Soils through Native Grass Cover in the Mt. Amiata Region of Italy. *Environmental Research* 2013, *125*, 69–74.
<https://doi.org/10.1016/j.envres.2013.02.004>.
28. US EPA, O. *Abandoned Mine Drainage*.
<https://www.epa.gov/nps/abandoned-mine-drainage> (accessed 2024-06-05).

29. Morillas, L.; Roales, J.; Cruz, C.; Munzi, S. Lichen as Multipartner Symbiotic Relationships. *Encyclopedia* 2022, 2 (3), 1421–1431.
<https://doi.org/10.3390/encyclopedia2030096>.
30. Landis, M. S.; Berryman, S. D.; White, E. M.; Graney, J. R.; Edgerton, E. S.; Studabaker, W. B. Use of an Epiphytic Lichen and a Novel Geostatistical Approach to Evaluate Spatial and Temporal Changes in Atmospheric Deposition in the Athabasca Oil Sands Region, Alberta, Canada. *Science of The Total Environment* 2019, 692, 1005–1021.
<https://doi.org/10.1016/j.scitotenv.2019.07.011>.
31. Garty, J. Biomonitoring Atmospheric Heavy Metals with Lichens: Theory and Application. *Critical Reviews in Plant Sciences* 2001, 20 (4), 309–371.
<https://doi.org/10.1080/20013591099254>.
32. Loppi, S.; Pacioni, G.; Olivieri, N.; Giacomo, D. Accumulation of Trace Metals in the Lichen Evernia Prunastri Transplanted at Biomonitoring Sites in Central Italy. *The Bryologist* 1998, 101, 451–454.
<https://doi.org/10.2307/3244187>.
33. Brown, D. H.; Rapsch, S.; Beckett, A.; Ascaso, C. The Effect of Desiccation on Cell Shape in the Lichen *Parmelia Sulcata* Taylor. 1987.
34. Bubach, D. F.; Pérez Catán, S.; Arribére, M. A.; Diéguez, M. C.; García, P. E.; Messuti, M. I. Mercury Content and Elemental Composition of Fruticose Lichens from Nahuel Huapi National Park (Patagonia, Argentina): Time

- Trends in Transplanted and *in Situ* Grown Thalli. *Atmospheric Pollution Research* 2024, 15 (2), 101988. <https://doi.org/10.1016/j.apr.2023.101988>.
35. Koz, B.; Celik, N.; Cevik, U. Biomonitoring of Heavy Metals by Epiphytic Lichen Species in Black Sea Region of Turkey. *Ecological Indicators* 2010, 10 (3), 762–765. <https://doi.org/10.1016/j.ecolind.2009.11.006>.
36. *Les Lichens Du Jardin Du Luxembourg*.
<https://www.tandfonline.com/doi/epdf/10.1080/00378941.1866.10827433?src=getftr> (accessed 2024-04-10).
37. Bargagli, R. Moss and Lichen Biomonitoring of Atmospheric Mercury: A Review. *Science of The Total Environment* 2016, 572, 216–231.
<https://doi.org/10.1016/j.scitotenv.2016.07.202>.
38. *Foliose Lichen - an overview | ScienceDirect Topics*.
<https://www.sciencedirect.com/topics/agricultural-and-biological-sciences/foliose-lichen> (accessed 2024-05-21).
39. Godinho, R. M.; Verburg, T. G.; Freitas, M. C.; Wolterbeek, H. T. Accumulation of Trace Elements in the Peripheral and Central Parts of Two Species of Epiphytic Lichens Transplanted to a Polluted Site in Portugal. *Environ Pollut* 2009, 157 (1), 102–109.
<https://doi.org/10.1016/j.envpol.2008.07.021>.
40. Nimis, P. L.; Purvis, O. W. Monitoring Lichens as Indicators of Pollution. In *Monitoring with Lichens — Monitoring Lichens*; Nimis, P. L., Scheidegger,

C., Wolseley, P. A., Eds.; Springer Netherlands: Dordrecht, 2002; pp 7–10.

https://doi.org/10.1007/978-94-010-0423-7_2.

41. Vannini, A.; Jamal, M. B.; Gramigni, M.; Fedeli, R.; Ancora, S.; Monaci, F.;

Loppi, S. Accumulation and Release of Mercury in the Lichen *Evernia*

Prunastri (L.) Ach. *Biology (Basel)* 2021, *10* (11), 1198.

<https://doi.org/10.3390/biology10111198>.

42. Chahloul, N.; Khadhri, A.; Vannini, A.; Mendili, M.; Raies, A.; Loppi, S.

Selecting the Species to Be Used in Lichen Transplant Surveys of Air

Pollution in Tunisia. *Environ Monit Assess* 2023, *195* (5), 570.

<https://doi.org/10.1007/s10661-023-11219-4>.

43. *Lexington Reservoir County Park - Parks and Recreation - County of Santa*

Clara. <https://parks.sccgov.org/santa-clara-county-parks/lexington-reservoir-county-park> (accessed 2024-04-16).

44. Straw, B. Lichen Bioindicators Reveal the Impacts of Atmospheric Mercury

in the New Almaden Mining District, UC Santa Cruz, 2023.

<https://escholarship.org/uc/item/0rj3h6r8> (accessed 2024-04-08).

45. *Overview*. Tekran Instruments Corporation.

<https://www.tekran.com/products/merpas/overview/> (accessed 2024-04-29).

46. Jeon, B.; Cizdziel, J. V. Can the MerPAS Passive Air Sampler Discriminate

Landscape, Seasonal, and Elevation Effects on Atmospheric Mercury? A

Feasibility Study in Mississippi, USA. *Atmosphere* 2019, *10* (10), 617.

<https://doi.org/10.3390/atmos10100617>.

47. *Enriched Ambient Air Sampling*. Tekran Instruments Corporation.
<https://www.tekran.com/products/merpas/high-level-sampling/> (accessed 2024-05-30).
48. US EPA, O. *EPA Method 7473 (SW-846): Mercury in Solids and Solutions by Thermal Decomposition, Amalgamation, and Atomic Absorption Spectrophotometry*. <https://www.epa.gov/esam/epa-method-7473-sw-846-mercury-solids-and-solutions-thermal-decomposition-amalgamation-and> (accessed 2024-04-23).
49. Brueseke, M. Milestone DMA-80, Tricell.
50. *R: The R Project for Statistical Computing*. <https://www.r-project.org/> (accessed 2024-06-04).
51. *Empirical Bayesian Kriging (Geostatistical Analyst)—ArcGIS Pro | Documentation*. <https://pro.arcgis.com/en/pro-app/latest/tool-reference/geostatistical-analyst/empirical-bayesian-kriging.htm> (accessed 2024-04-24).
52. Gačnik, J.; Živković, I.; Kotnik, J.; Božič, D.; Tassone, A.; Naccarato, A.; Pirrone, N.; Sprovieri, F.; Steffen, A.; Horvat, M. Comparison of Active Measurements, Lichen Biomonitoring, and Passive Sampling for Atmospheric Mercury Monitoring. *Environ Sci Pollut Res Int* 2024, 31 (24), 35800–35810. <https://doi.org/10.1007/s11356-024-33582-6>.

53. *CLU-IN | Contaminants > Mercury > Chemistry and Behavior*. https://clu-in.org/contaminantfocus/default.focus/sec/Mercury/cat/Chemistry_and_Behavior/ (accessed 2024-06-05).